Basin Research (2004) **16**, 297–324, doi: 10.1111/j.1365-2117.2004.00234.x

The Marinoan glaciation (Neoproterozoic) in northeast Svalbard

Galen P. Halverson, Adam C. Maloof and Paul F. Hoffman

Department of Earth and Planetary Sciences, Harvard University, Cambridge, Massachusetts, USA

ABSTRACT

Two separate and distinct diamictite-rich units occur in the mixed carbonate-siliciclastic Polarisbreen Group, which comprises the top kilometer of >7 km of Neoproterozoic strata in the northeast of the Svalbard archipelago. The platformal succession accumulated on the windward, tropical to subtropical margin of Laurentia. The older Petrovbreen Member is a thin glacimarine diamictite that lacks a cap carbonate. It contains locally derived clasts and overlies a regional karstic disconformity that was directly preceded by a large (>10‰) negative $\delta^{13}C$ anomaly in the underlying shallow-marine carbonates. This anomaly is homologous to anomalies in Australia, Canada and Namibia that precede the Marinoan glaciation. The younger and thicker Wilsonbreen Formation comprises terrestrial ice-contact deposits. It contains abundant extrabasinal clasts and is draped by a transgressive cap dolostone 3–18 m thick. The cap dolostone is replete with sedimentary features strongly associated with post-Marinoan caps globally, and its isotopic profile is virtually identical to that of other Marinoan cap dolostones. From the inter-regional perspective, the two diamictite-rich units in the Polarisbreen Group should represent the first and final phases of the Marinoan glaciation. Above the Petrovbreen diamictite are $\sim$200 m of finely laminated, dark olive-coloured rhythmites (MacDonaldryggen Member) interpreted here to represent suspension deposits beneath shorefast, multi-annual sea ice (sikussak). Above the suspension deposits and below the Wilsonbreen diamictites is a <30-m-thick regressive sequence (Slangen Member) composed of dolomite grainstone and evaporitic supratidal microbialaminite. We interpret this sabkha-like lagoonal sequence as an oasis deposit that precipitated when local marine ice melted away under greenhouse forcing, but while the tropical ocean remained covered due to inflow of sea glaciers from higher latitudes. It appears that the Polarisbreen Group presents an unusually complete record of the Marinoan snowball glaciation.

INTRODUCTION

In the northeastern part of the Svalbard archipelago, a Caledonian (Silurian) fold belt exposes a magnificent 7-km-thick succession of Neoproterozoic through Middle Ordovician sedimentary strata (Fig. 1). The Hecla Hoek Succession (Harland & Wilson, 1956; Knoll & Swett, 1990; Harland *et al*., 1993) is similar to that in the East Greenland Caledonides (Hambrey & Spencer, 1987; Sønderholm & Tirsgaard, 1993; Fairchild & Hambrey, 1995), and they jointly formed a platform contiguous with the windward, tropical to subtropical margin of Laurentia (Fig. 1). The late Neoproterozoic Polarisbreen Group (Fig. 1) sits atop 2 km of conformable carbonate strata, the Akademikerbreen Group, and within its mixed terrigenous and carbonate sequences are two separate and distinct glacial diamictite-rich units (Harland *et al*., 1993).

It is now widely accepted that at least one large Neoproterozoic ice sheet reached tidewater close to the equator (Embleton & Williams, 1986; Schmidt & Williams, 1995; Sohl *et al*., 1999; Evans, 2000) – a climatic scenario that cannot be understood in terms of Quaternary analogues. Invoking various lines of geological and geochemical evidence, as well as simple energy-balance climate models (e.g. Budyko, 1969; Sellers, 1969; Caldeira & Kasting, 1992), Kirschvink (1992), Klein & Beukes (1993) and Hoffman *et al*. (1998) proposed that the entire ocean froze over during the Sturtian and Marinoan ice ages.

Much attention focused on marine sedimentary and isotopic proxy records of the conditions under which low-latitude glaciation was initiated (Halverson *et al*., 2002; Schrag *et al*., 2002) and later terminated (Fairchild, 1993; Grotzinger & Knoll, 1995; Kennedy, 1996; Hoffman *et al*., 1998; Kennedy *et al*., 1998; James *et al*., 2001; Hoffman & Schrag, 2002; Higgins & Schrag, 2003). In three of the best-studied regions, the Adelaide rift complex in South Australia, the northern Canadian Cordillera, and the Congo cratonic margin in Namibia, the deposits associated with the younger (Marinoan) glacials are directly underlain by an unique carbon isotope anomaly (McKirdy *et al*., 2001; Halverson *et al*., 2002; Hoffman & Schrag, 2002), and are directly overlain by a lithologically unique cap-carbonate sequence (Kennedy, 1996; Soffer, 1998; James *et al*., 2001; Hoffman & Schrag, 2002). The older glacial sequence

Correspondence: Galen P. Halverson, Department of Earth and Planetary Sciences, Harvard University, 20 Oxford St., Cambridge, MA 02138, USA. E-mail: halvers@eps.harvard.edu

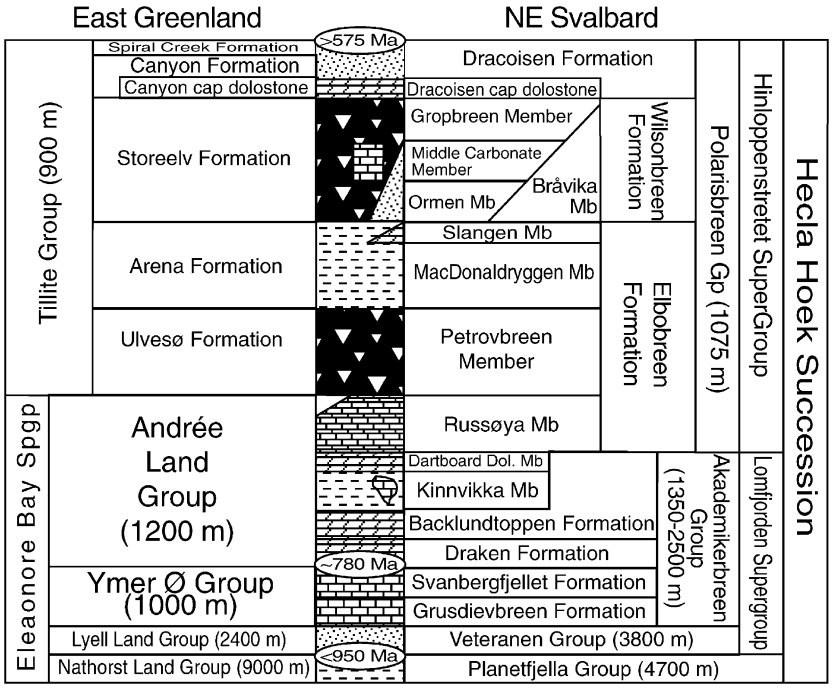

Fig. 1. Generalized lithostratigraphy of the Proterozoic successions in northeast Svalbard (Harland *et al.*, 1966; Fairchild & Hambrey, 1984; Knoll & Swett, 1990; this paper) and East Greenland (Katz, 1960; Henriksen & Higgins, 1976; Hambrey & Spencer, 1987; Herrington & Fairchild, 1989; Sønderholm & Tirsgaard, 1993; Frederiksen *et al.*, 1999; Smith & Robertson, 1999a). Correlations between East Svalbard and East Greenland are based on original lithological (e.g. Harland *et al.*, 1993; Fairchild & Hambrey, 1995) and carbon-isotopic (e.g. Knoll *et al.*, 1986) comparisons from the literature. Black regions denote glacial diamictites. The maximum age of 950 Ma for the Veteranen Group is based on U-Pb dating of detrital zircons from NE Spitsbergen (Larionov *et al.*, 1998) and igneous zircons from sub-Veteranen Group granites in Nordaustlandet (Gee *et al.*, 1995). The 780 Ma age for the Svanbergfjellet-Draken formations is a loose approximation based on biostratigraphic correlations with Australia (Hill *et al.*, 2000) and an unpublished Rb-Sr isochron (S. Jacobsen, pers. comm.) on the middle Grusdievbreen Formation. The 575 Ma minimum age for the top of the succession is based on the absence of Ediacaran fossils in Svalbard and East Greenland (Knoll & Swett, 1987) and an age of ~575 Ma for the oldest known Ediacaran fossils, in Newfoundland (Bowring *et al.*, 2003).

has no similar premonitory isotope anomaly and its cap-carbonate sequence is isotopically and lithologically unlike the Marinoan cap (Kennedy *et al.*, 1998). Accordingly, pre- and post-glacial strata in combination should offer a more reliable basis for correlation than the glacial deposits alone, which are usually discontinuous and spatially variable.

Here we present detailed stratigraphic and geochemical data spanning what previously were regarded as two discrete glaciations in the Polarisbreen Group (Hambrey, 1982; Knoll *et al.*, 1986; Harland *et al.*, 1993; Fairchild & Hambrey, 1984, 1995; Kaufman *et al.*, 1997). The glacial units are different lithologically and the younger one (Wilsonbreen Formation) has a cap-carbonate sequence (basal Dracoisen Formation) indistinguishable from other Marinoan cap carbonates. On the other hand, the sub-Marinoan isotope anomaly consistently appears beneath the older glacial unit (Petrovbreen Member) and never beneath the younger glacials. Two interpretations are possible. Either the correlation criteria developed in Australia, Canada and Namibia are faulty, or both glacial units in Svalbard plus the intervening strata (including open-water lagoonal deposits) belong to a single Marinoan glaciation. In this paper, we explore the latter interpretation and attempt to reconcile it with evidence from elsewhere that the Marinoan glaciation was a snowball cycle (Kirschvink, 1992; Hoffman *et al.*, 1998; Hoffman & Schrag, 2002). We briefly discuss the implications of our proposed correlations for the Sturtian glaciation in Svalbard.

GEOLOGICAL BACKGROUND

The Polarisbreen Group (Fig. 1) comprises the mixed siliciclastic-carbonate Elbobreen, Wilsonbreen and Dracoisen Formations in the uppermost Neoproterozoic of the Hecla Hoek Succession of northeastern Spitsbergen (Wilson & Harland, 1964; Fairchild & Hambrey, 1984). It conformably overlies a thick carbonate platform, the Akademikerbreen Group, which grades downward into siliciclastic strata of the underlying Veteranen Group (Fig. 1). A cryptic unconformity separates the Polarisbreen Group from the Cambrian Tokammane Formation (Harland *et al.*, 1993), but biostratigraphy suggests a significant hiatus (Knoll & Swett, 1987). The Polarisbreen Group is exposed in a north-south trending belt that extends from southern

Olav V Land in Spitsbergen to western Nordaustlandet (Fig. 2). A different stratigraphic nomenclature was defined in Nordaustlandet, but as correlation with Spitsbergen is unambiguous (Harland & Gayer, 1972; Knoll *et al.*, 1986; Fairchild & Hambrey, 1995), the Spitsbergen nomenclature (Fig. 1) will be used throughout this paper. Three informal names are proposed for established members.

The older glacigenic unit in the Polarisbreen Group is the Petrovbreen Member (Harland *et al.*, 1993) of the Elbobreen Formation (Fig. 3). Younger and typically much thicker glacigenic diamictites make up the Wilsonbreen Formation (Fig. 3). The glacial units have been studied sedimentologically (Chumakov, 1968; Hambrey, 1982; Fairchild & Hambrey, 1984; Harland *et al.*, 1993) and geochemically (Fairchild & Spiro, 1987, 1990; Fairchild *et al.*, 1989). They are often correlated with Neoproterozoic diamictite pairs in other parts of the North Atlantic region (e.g. Hambrey, 1983; Nystuen, 1985; Fairchild & Hambrey, 1995), but geochronological confirmation is lacking. The correlation with the Tillite Group in East Greenland (Fig. 1) is the most widely accepted (Kulling, 1934; Harland & Gayer, 1972; Knoll *et al.*, 1986; Hambrey & Spencer, 1987; Fairchild & Hambrey, 1995). The Neoproterozoic successions in eastern Svalbard and East Greenland are similar in their entirety (Fig. 1) and there is consensus that they formed in contiguous sedimentary basins. Knoll *et al.* (1986) produced an early record of the secular variation of $\delta^{13}C$ in carbonate and organic matter carbon in the two successions, which supported the correlation and drew attention to the connection between Neoproterozoic glaciations and large negative $\delta^{13}C$ anomalies. Fairchild & Spiro (1987) and Kaufman *et al.* (1997) have since provided additional isotopic data for Polarisbreen Group carbonates, including stromatolitic limestones within the Wilsonbreen glacials. The data presented here confirm and build upon this previous work.

Tectonic setting

The Svalbard archipelago comprises three tectonic terranes that were juxtaposed through sinistral transpression during the Silurian–Devonian Ny Friesland orogeny (Harland & Gayer, 1972; Harland *et al.*, 1992; Gee & Page, 1994; Lyberis & Manby, 1999; Dewey & Strachan, 2003). The Hecla Hoek Succession (Neoproterozoic–Middle Ordovician) underlies the northern part of the eastern terrane, which includes parts of the Barents Sea and is called Barentsia. The correlation of the Hecla Hoek with the succession in the southern East Greenland Caledonides (Fig. 1) underpins the consensus view that Barentsia originated on the Laurentian margin adjacent to East Greenland (Harland & Gayer, 1972), forming part of a joint East Greenland–East Svalbard (EGES) platform. The origin of the EGES platform is obscure, but presumably it was associated with the fragmentation of Rodinia, which in the region of the EGES platform involved the separation of four cratons

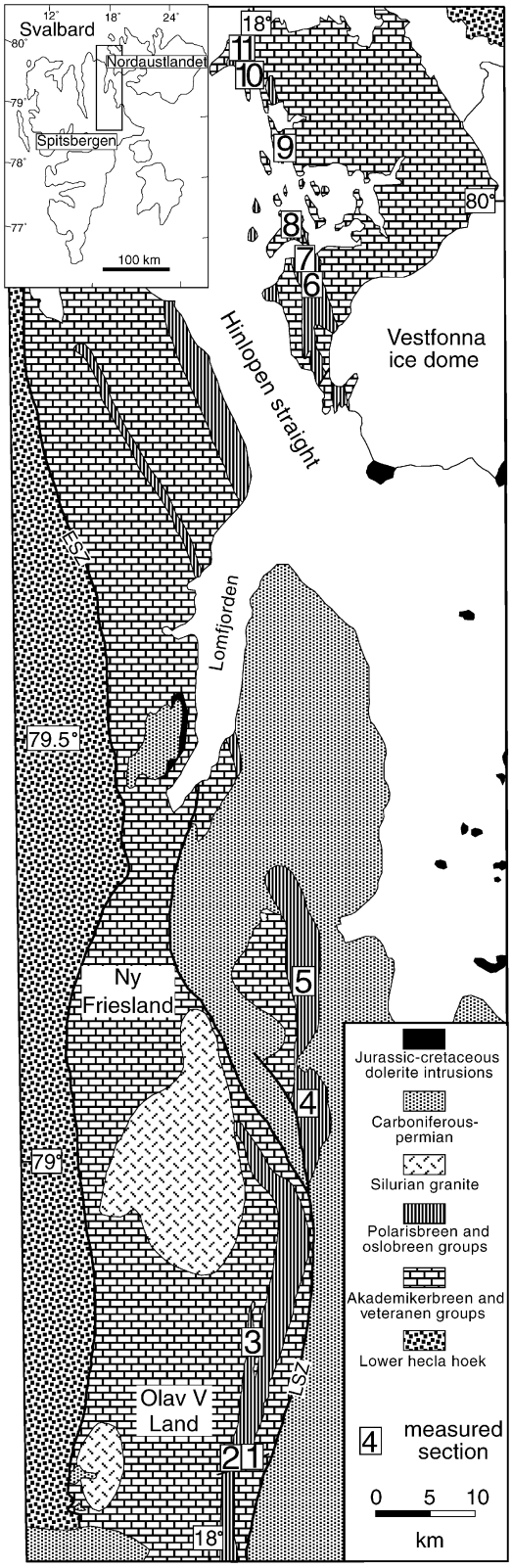

Fig. 2. Geological map of the north–south trending Neoproterozoic outcrop belt in northeastern Svalbard (Olav V Land, Ny Friesland, and northwestern Nordaustlandet). Numbered boxes key measured sections in Figs 4 and 8. See the Supplementary material for location names and coordinates. ESZ = Eolussletta Shear Zone; LFZ = Lomfjorden Fault Zone. Location names: (1) Backlundtoppen, (2) Slangen-Ormen, (3) Klofjellet, (4) Ditlovtoppen, (5) Dracoisen, (6) Liljequisthøgda, (7) Sveanor, (8) Søre Russøya, (9) Kinnvikka, (10) Bråvika and (11) Skyttelodden.

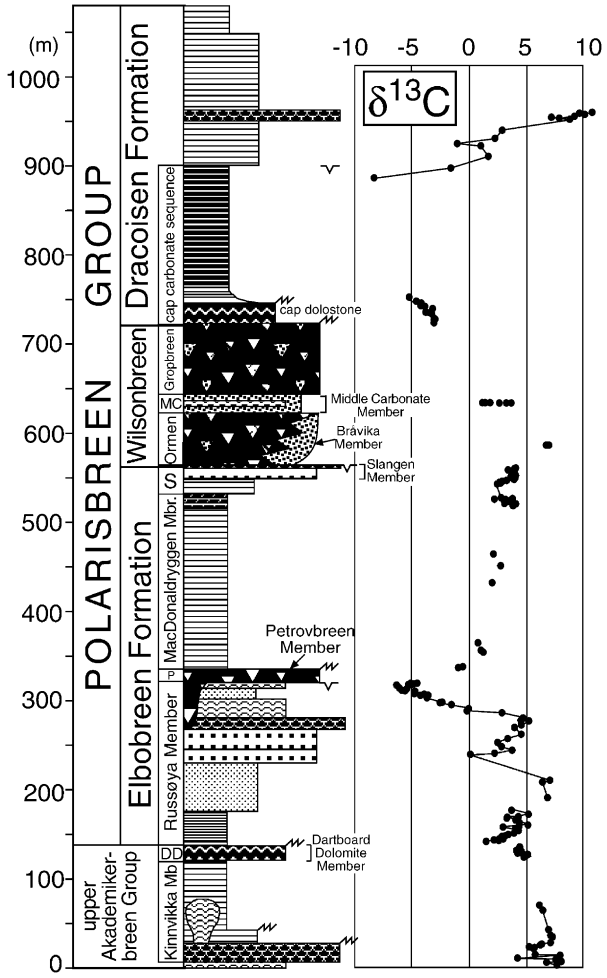

Fig. 3. Composite stratigraphic and $\delta^{13}C$ profile through the Polarisbreen Group. See text for discussion of how the composite was constructed and Fig. 4 for the legend.

including Laurentia, Baltica, and Amazonia (Torsvik *et al.*, 1996; Hartz & Torsvik, 2002).

The north–south trending outcrop belt in northeast Svalbard (Fig. 2) is believed roughly to parallel the East Greenland cratonic margin (Knoll & Swett, 1990; Fairchild & Hambrey, 1995). Following the siliciclastic Veteranen Group (>4 km), a broad carbonate platform (Akademikerbreen Group) developed (Fig. 1). The conformable nature of the 2-km-thick carbonate succession suggests broad thermal subsidence, and the paucity of terrigenous input implies either a subtropical location with little runoff or a semi-isolated platform like the Bahamas. The strata thin northward, particularly in the upper Svanbergfjellet and Draken Formations (Wilson, 1961), consistent with a southerly opening basin (Hartz & Torsvik, 2002). Renewed crustal stretching is inferred from deepening of the platform in East Greenland (Herrington & Fairchild, 1989) and an influx of fine terrigenous sediment (Kinnvikka Member, Fig. 1) in the uppermost Backlundtoppen Formation (Fairchild & Hambrey, 1995), although we postulate an additional paleoclimatic factor at this time. The Polarisbreen Group is dominantly siliciclastic (Fig. 3), but shallow-water carbonate banks were intermittently reestablished (Fairchild & Hambrey, 1995).

Paleopoles constrain the paleogeographic position of Laurentia at 723 Ma (Franklin Dikes; Buchan *et al.*, 2000; Heaman *et al.*, 1992) and 615 Ma (Long Range Dikes; Murthy *et al.*, 1992; Kamo & Gower, 1994), but the apparent polar wander path between those ages is unconstrained. Both poles place the EGES platform in low southern latitudes, with the East Greenland margin facing the southeasterly trade winds and the depositional strike of the basin trending roughly southwest–northeast. During parts of this interval, the margin may have been under the influence of the dry downwelling arm of the Hadley circulation, and onshore trade winds (from the present-day northeast) may have dominated the margin throughout.

Geochronology

Precise ages from the Neoproterozoic of Svalbard are lacking. The only firm age constraint is a maximum of ~950 Ma for the base of the Veteranen Group from detrital zircons in the upper Planetfjella Group (Fig. 1) in Ny Friesland (Larianov *et al.*, 1998) and primary zircons in the underlying granites in northern Nordaustlandet (Gee *et al.*, 1995; Johannson *et al.*, 2000). The lack of Ediacaran fossils in the Polarisbreen (Knoll & Swett, 1987) suggests a minimum age of ~575 Ma (Bowring *et al.*, 2003). Derry *et al.* (1992) applied a time line to the Neoproterozoic stratigraphy based on a single, unpublished Rb–Sr isochron (~780 Ma) in the lower Akademikerbreen Group (Grusdievbreen Formation; S. Jacobsen, pers. comm., 2002) and correlation with the Shaler Group in northern Canada (Asmeron *et al.*, 1991). Derry *et al.* (1992) estimated an age of 630 Ma for the base of the Polarisbreen, but this age hinges on correlation with other poorly dated Neoproterozoic glaciations. Hill & Walter (2000) suggested an age of ~780 Ma for the Svanbergfjellet Formation (Fig. 1) based on the occurrence of the acritarch *Cerebrosphaera buickii* in both the Svanbergfjellet and Draken formations in Svalbard (Knoll *et al.*, 1991; Butterfield *et al.*, 1994) and the middle Burra Group in South Australia (Cotter, 1999; Hill *et al.*, 2000), the base of which is dated at 777 ± 7 Ma (Preiss, 2000).

METHODS

Sample selection and preparation

All samples were collected in the course of measuring stratigraphic sections. Fresh dolomite and limestone samples with little visible veining, cleavage or siliciclastic component were targeted. Samples were prepared by cutting slabs perpendicular to lamination and polishing one face to clear saw marks and clarify internal texture. Between 5 and 20 mg of powder were microdrilled from the individual laminations (where visible) on the polished slab, collected and stored. All subsequent isotopic and elemental analyses were performed on aliquots of this powder.

Isotopic analysis

$\delta^{13}C$ and $\delta^{18}O$ isotope data (see the Supplementary material) were acquired simultaneously on a VG Optima dual inlet mass spectrometer attached to a VG Isocarb preparation device (Micromass, Milford, MA, USA) in the Harvard University Laboratory for Geochemical Oceanography. Approximately, 1-mg microdrilled samples were reacted in a common, purified H_3PO_4 bath at 90 °C. Evolved CO_2 was collected cryogenically and analysed using an in-house reference gas. External error (1σ) from standards was better than $\pm$ 0.1‰ for both $\delta^{13}C$ and $\delta^{18}O$. Samples were calibrated to VPDB using the Cararra Marble standard. Potential memory effect resulting from the common acid-bath system was minimized by tripling the reaction time for dolomite samples. Memory effect is estimated at $<$0.1‰ based on variability of standards run after dolomite samples.

Elemental analyses

Elemental analyses (Ca, Mg, Sr, Mn, Fe, Na) were performed on a Jovin Yvon 46P ICP-AES mass spectrometer in the Harvard University Laboratory for Geochemical Oceanography. All samples were prepared by dissolving $\sim$4 mg of carbonate powder in $\sim$4 ml of 2% nitric acid. SCP multielement standards were used for element-specific calibration at the beginning of each run. External error (1σ), determined by repeat analyses, was $<$7% for all elements other than Na, which had an error of $\sim$28% and is regarded as only an approximate figure.

RESULTS AND INTERPRETATIONS

Here we summarize the stratigraphic, sedimentological, and $\delta^{13}C$ (carbonate) records in northeastern Svalbard, beginning with the first influx of terrigenous sediments in the upper Backlundtoppen Formation (Fig. 1) and ending with the cap-carbonate sequence (Dracoisen Formation) above the Wilsonbreen glacials. We introduce informal names for three previously unnamed members, as shown in Fig. 3: the Kinnvikka Member (Member B5 of Harland, 1997) of the Backlundtoppen Formation, the Russøya (E1 of Harland *et al.*, 1993) Member of the Elbobreen Formation, and the Bråvika Member of the Wilsonbreen Formation.

Figure 3 presents a composite stratigraphic section constructed so as to provide the most complete isotopic coverage available, using splices of the upper Backlundtoppen Formation at Bråvika (measured section 10); the lower Russøya Member at Backlundtoppen (measured section 1) and Sveanor (measured section 7); the upper Russøya Member at Sveanor (measured section 7); the Petrovbreen Member through Wilsonbreen Formation at Dracoisen (measured section 5, including our only complete section of the MacDonaldryggen Member); and the Dracoisen Formation at Ditlovtoppen (measured section 4). Significant erosional relief is present at the base of the Petrovbreen diamictite, but the underlying Russøya Member appears to be nearly complete in most Nordaustlandet sections. No other prominent erosional truncation (excluding that beneath the contact with the Cambrian) is apparent. Thus, the main gaps in the isotopic record correspond to the two glacial intervals and siliciclastics in the upper Kinnvikka Member, the MacDonaldryggen Member, and in the Dracoisen Formation.

Kinnvikka Member

The upper Backlundtoppen Formation is an $\sim$200-m-thick stack of uninterrupted stromatolites (Wilson, 1961; Knoll *et al.*, 1989; Knoll & Swett, 1990) that is strongly enriched isotopically ($\delta^{13}C \approx 8$‰; Fig. 4a). This unit is locally capped by a bed of irregular and discontinuous microbially laminated dolomite (microbialaminites) with tepee structures, indicating emergence and the end of the long-lived Akademikerbreen carbonate platform. A flooding surface above this microbialaminite bed marks the base of what is defined here as the Kinnvikka Member. The lower part of the Kinnvikka Member is a 5–20-m-thick interval of thin parasequences of shales, ribbon carbonates (ribbonites), and microbialaminites. The carbonates at the base of the Kinnvikka Member are less ^{13}C-enriched ($\delta^{13}C \approx 5$‰) than the underlying stromatolites. Above this interval is another prominent flooding surface. In most sections, the overlying strata form a fining- then coarsening-upward parasequence (15–40+ m) of predominantly shale, siltstone and fine sandstone. Lesser green shales and dolomite breccia lenses occur within the siliciclastic interval.

At Bråvika (measured section 10), the northernmost measured section of this interval, a stromatolitic pinnacle reef, whose upward growth apparently kept up with the flooding of the underlying carbonates, protrudes from the lower carbonates well into the silty interval. This 45-m-high reef fortuitously documents marine carbon-isotopic composition of 5–7‰ through the lower Kinnvikka Member (Fig. 4b). Wedges of stromatolites, intraclast breccia, and muddy debris flows with dolomite clasts extend laterally into the siltstones, capping m-scale coarsening-upward cycles. Significant relief on the upper contact of the Kinnvikka dolostones in the Murchisonfjord area suggests that such reefs may be a common feature. These isolated stromatolite buildups likely supplied the dolomitic detritus in other lower Kinnvikka sections and may partly account for the highly variable thickness of the overlying siliciclastic interval. The inter-reef and upper Kinnvikka Member sediments are typically recessive-weathering, but based on float appear to consist of red argillite with minor sandstone, dolomitic breccia and grainstone. The nature of the contact with the overlying Dartboard Dolomite is uncertain due to poor exposure.

Dartboard Dolomite Member

The Dartboard Dolomite Member (Fig. 3) forms the top of the Akademikerbreen Group (Wilson, 1961; Wilson &

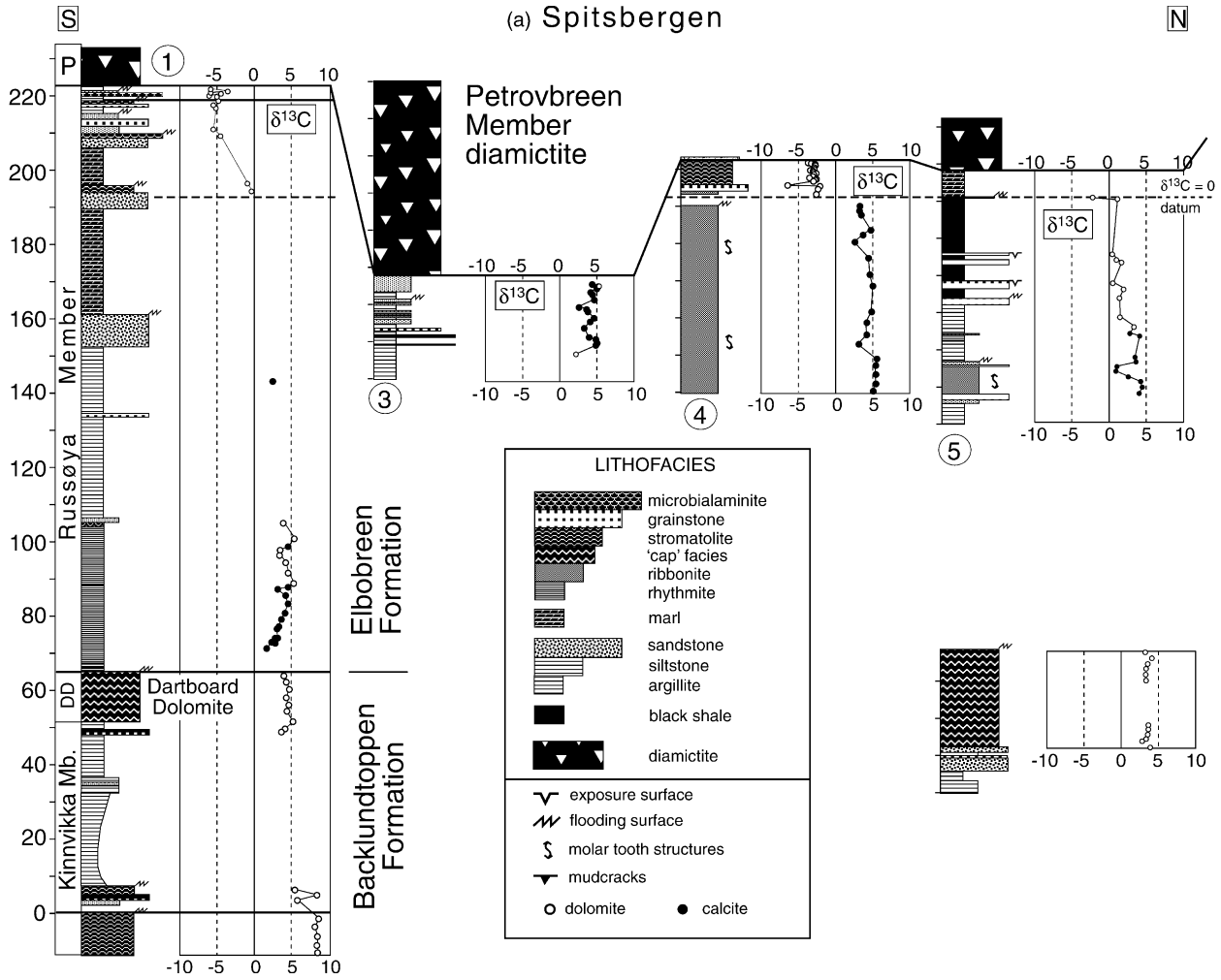

Fig. 4. Stratigraphic columns and corresponding $\delta^{13}C$ data (in per mil units vs. VPDB) for the Kinnvikka through Petrovbreen Members in Spitsbergen (a) and Nordaustlandet (b). Each column is hung on a $\delta^{13}C = 0$ datum (dashed line) where data is available (approximated where no or insufficient data are available) for the pre-Petrovbreen negative anomaly. The choice of this datum implies that the time at which $\delta^{13}C$ equaled 0‰ was the same everywhere in the basin, although this assertion is not proven. Hanging the stratigraphic columns on this datum demonstrates what we interpret to be variable erosional truncation of the upper Russøya Member, and we note that the implied depth of erosion roughly correlates with the thickness of the Petrovbreen Member diamictite (e.g. measured section 3). Solid lines show correlation of the base of the Kinnvikka Member, top of the Dartboard Dolomite Member, and the base of the upper parasequence of the Russøya Member. Gaps in stratigraphic coverage represent unexposed section. See the Supplementary material for tabulated $\delta^{18}O$ and $\delta^{13}C$ data.

Harland, 1964) and occurs throughout the outcrop belt except at its northernmost exposure in Ny Friesland (Kluftdalen). Elsewhere in Ny Friesland and Olav V Land, the Dartboard Dolomite is ~25 m thick, commonly stromatolitic, typified by lobate–cuspate laminations, and pervasively recrystallized and vuggy (Fairchild & Hambrey, 1984). In some exposures, the stromatolites are laterally linked and steep-walled with synoptic relief of up to 3 m and, in plan view, define concentric patterns of laminations (hence the name 'Dartboard'), reminiscent of *Conophyton* (Knoll *et al.*, 1989). In other exposures, the cuspate structures are nearly vertical, disrupted and brecciated at the apex (Fairchild & Hambrey, 1984), and linear to irregular in plan view. These structures more closely resemble peritidal tepees (cf. Kendall & Warren, 1987) than coniform stromatolites, and indicate deposition on a shallow, episodically desiccated platform (Fairchild & Hambrey, 1984). The upper contact of the Dartboard Dolomite is brecciated at measured section 1 and in several other Ny Friesland sections (Fairchild & Hambrey, 1984).

The Dartboard Dolomite Member is superficially similar in Nordaustlandet exposures, but sedimentologically distinct and not as pervasively recrystallized. At Kinnvikka (measured section 10, Fig. 4b), the entire unit is 16 m thick and its base consists of tightly packed peloids and breccias with abundant, isopachous, void-filling cements (Fig. 5a). Up section, macropeloids and microbial laminae are increasingly interbedded. As microbial laminae becomes predominant, it forms broad domes with intervening, peloid-filled, and occasionally bridges troughs. In the upper half of the unit, continuous microbial laminae form wave-like bedforms with meter-scale amplitude and

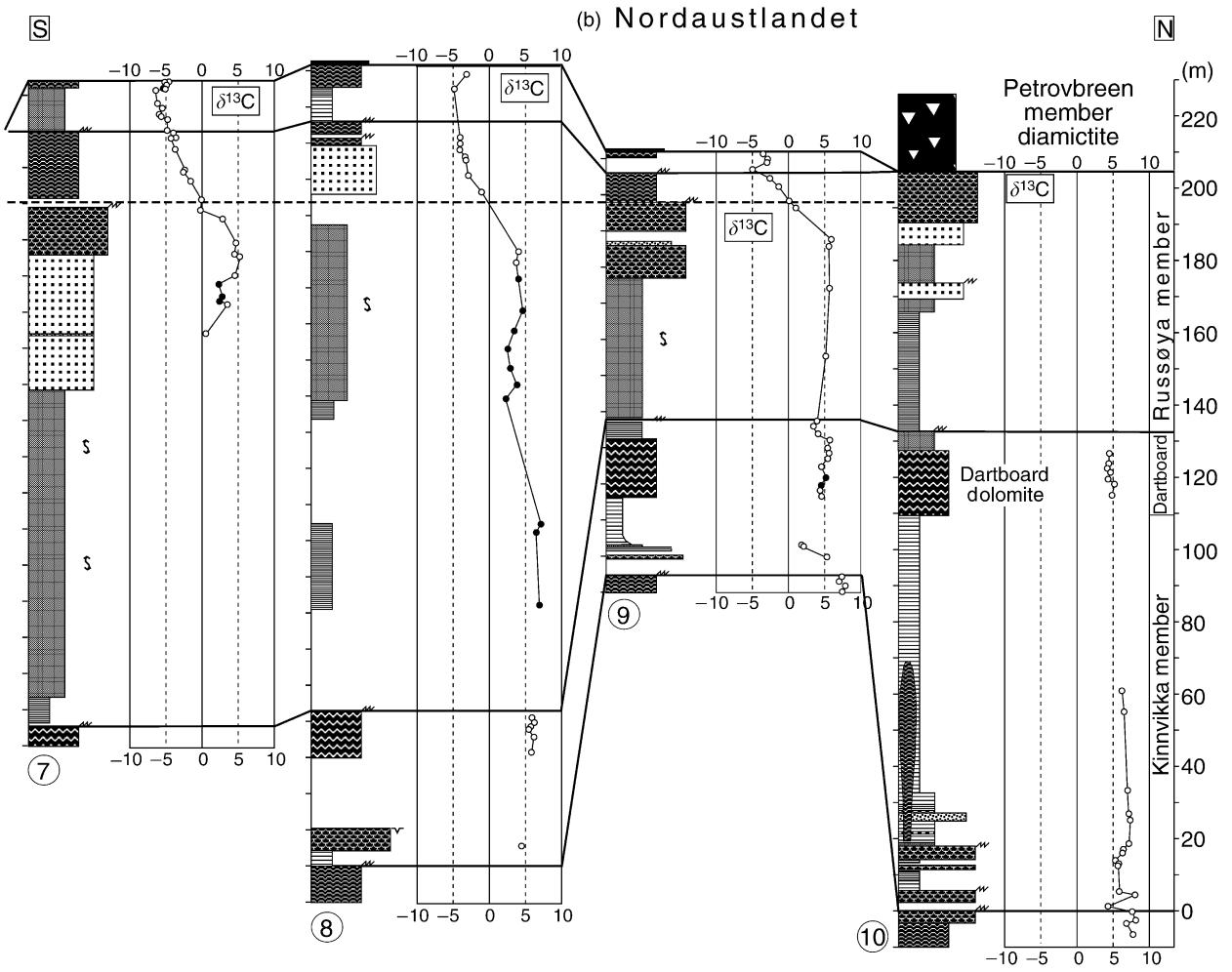

Fig. 4. (Continued)

wavelength. Geometrically, the structures resemble tepees, with broad troughs and pinched crests that intersect to form a quasi-orthogonal grid in plan view. However, distinct from the Ny Friesland examples, these structures are neither disrupted nor brecciated, and no other evidence points to a shallow-water or intermittently emergent environment. Enigmatically, whereas the lamination appears more consistent with sediment stabilized by microbial mats, the bedforms are more compatible with traction transport of granular sediment. The microbial lamination flattens, and the dolomite becomes ferroan toward the top of the unit, which in Nordaustlandet appears gradational with the overlying Russøya Member.

$\delta^{13}C$ through the Dartboard Dolomite Member consistently ranges from 3‰ to 6‰, but shows no discernible trend up section (Fig. 4). Nor does $\delta^{13}C$ vary noticeably between individual sections, despite facies variations and the evidence for extensive alteration in Ny Friesland.

Russøya Member

The poorly exposed lower part of the Russøya Member is variable in thickness and facies, but forms a distinct upward-shoaling sequence 45–135 m thick. At Backlundtoppen (measured section 1), the brecciated contact of the upper Dartboard is overlain by 3 m of black shale, followed by 26 m of bluish-grey to black limestone rhythmites with increasing proportions of thin dolomite beds upwards. The carbonates grade upward into dark, marly shales with peculiar, crinkly microbial laminae. The sequence is capped by a 7.5 m-thick, poorly sorted, coarse-grained sandstone. Elsewhere in Spitsbergen, the upper part of the sequence is more organic-rich and its top surface is not easily identified (Fig. 4a). In Nordaustlandet, the lower Russøya Member appears continuous with the Dartboard Dolomite, where microbial laminae below pass upward into dolomitic, then heavily silicified rhythmites beneath a poorly exposed interval of marly black shale, rhythmites, and limestone ribbonites with molar tooth structures. This thick (up to 110 m), relatively deep-water interval shoals upward into grainstones and microbialaminites, with an occasional thin sandstone bed.

The upper Russøya Member is well exposed at Backlundtoppen (measured section 1), Dracoisen (measured section 4) and in several locations in Nordaustlandet (Fig. 4). In Ny Friesland (Fig. 4a), it comprises a series of 5–10-m

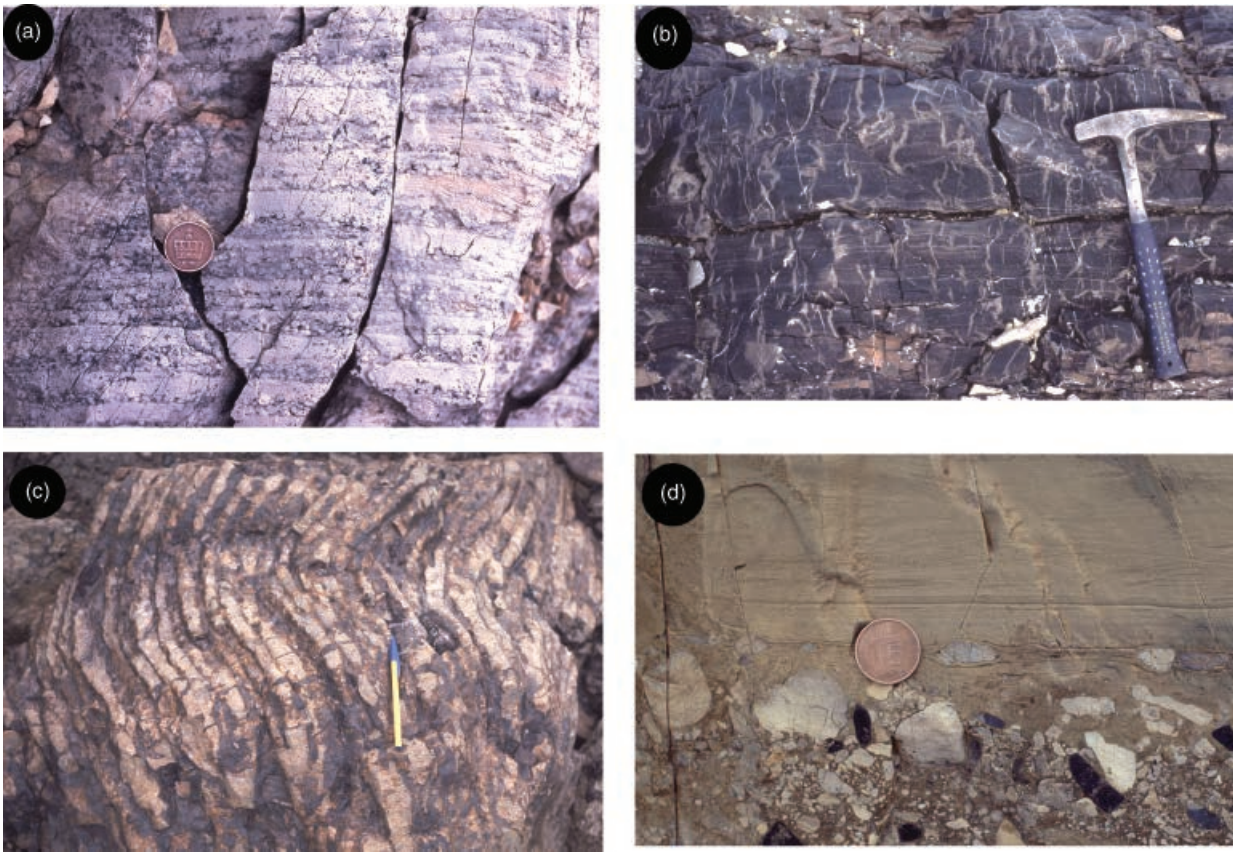

Fig. 5. Distinctive lithofacies in the Dartboard Dolomite Member of the Backlundtoppen Formation and the Russøya and Petrovbreen members of the Elbobreen Formation. (a) coarse peloids in a microbially laminated framework (the coin, for scale is the same size as a penny) at measured section 9, (b, c) Lithofacies of the upper Russøya Member: (b) Pervasive molar tooth structure in black limestone ribbonites at measured section 4, (c) *Kussiella* sp. biostrome at the top of the uppermost parasequence at measured section 9. (d) Petrovbreen Member: massive diamictite overlain by ripple cross-laminated dolarenite at measured section 5. Note predominance of angular dolomite (light grey) and chert (black) clasts, typical of the Petrovbreen Member (Harland *et al*., 1993).

thick cycles that variable consist of shale, black shale, or black limestone at the base and sandstone or dolomite grainstone at the top. Molar tooth structures (Fig. 5b) are common in the black limestone and are locally extremely dense, comprising up to 25% of the total rock mass. Large (up to 5-cm diameter) pyrite nodules occur locally in the black shales. Interbedded dolomites are typically iron-stained and vuggy and in places contain gypsum casts and silicified anhydrite nodules (Fairchild & Hambrey, 1984; Harland *et al*., 1993). Up section, the carbonate phase is exclusively dolomite. The uppermost Russøya consists of an assortment of facies, including m-scale biohermal stromatolite mounds (Fairchild & Hambrey, 1984), and is highly variable between sections. At Ditlovtoppen, the upper Russøya is condensed ($\sim$10 m) and is capped by a distinctive columnar stromatolite biostrome. In Nordaustlandet (Fig. 5b), the upper Russøya is thinner ($<$40 m) and less variable than in Ny Friesland. It consists of two parasequences, the lower of which is topped by biohermal stromatolites or microbialaminites. The upper parasequence is capped by a 2–6 m-thick biostrome (*Kussiella* sp.; Fig. 5c), nearly identical to that at Ditlovtoppen, but with collectively spiraling columns. The top of this parasequence is brecciated and variably truncated on the outcrop-scale.

The lower and upper Russøya have very different $\delta^{13}C$ trajectories (Figs. 3 and 4). The lower Russøya hovers around 5‰ through most of its thickness, following an initial rise from $\sim$1.5‰ near the base of the member at Backlundtoppen (measured section 1). In contrast, the upper Russøya declines from 5‰ to $-$6‰ just below the Petrovbreen diamictite. In Nordaustlandet, the decline begins beneath the penultimate parasequence (Fig 4b), and spans multiple facies, indicating that the anomaly does not record a surface-to-deep $\delta^{13}C$ gradient. In some Nordaustlandet sections, regarded here as the most complete, an upturn towards less negative values is preserved in the upper parasequence. In contrast, the anomaly is missing altogether in some Spitsbergen locations (measured sections 3 and 5; Fig. 4).

Petrovbreen Member diamictite

The Petrovbreen Member diamictite is typically thin ($\sim$10 m on average; Harland *et al*., 1993) and present nearly everywhere above the Russøya Member (Fig. 4). The Petrovbreen Member is generally thicker in Ny Friesland, with the thickest section (52 m) at Klofjellet (measured section 3). The Petrovbreen Member had previously

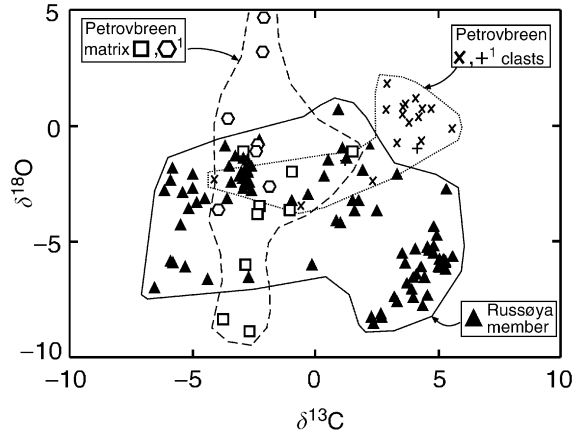

Fig. 6. $\delta^{13}C$–$\delta^{18}O$ cross-plot of Russøya carbonates and Petrovbreen Member matrix and clasts. The field of both the diamictite matrix and clasts generally overlap with the values from the underlying Russøya Member, although $\delta^{18}O$ values are more spread out [which Fairchild *et al.* (1989) interpret to represent a spectrum from least-altered ($\delta^{18}O > 0$‰) to most-altered ($\delta^{18}O < -5$‰) rock flour], and indicate that the Russøya Member was the predominant source of clasts to the Petrovbreen diamictite. [1]Data from Fairchild *et al.* (1989).

been reported from only one locality on Nordaustlandet (measured section 11; Hambrey, 1982; Harland *et al.*, 1993), but a thin and patchily preserved diamictite is found in most well exposed sections in Nordaustlandet.

In most sections, the bulk of the Petrovbreen Member consists of tan and yellow-weathering dolomitic rhythmites, finely laminated and rippled wackestone, and poorly sorted to massive diamictite (Fairchild & Hambrey, 1984). At Dracoisen (measured section 5), a ripple cross-laminated grainstone with outsized clasts comprises the uppermost part of the diamictite (Fig. 5d). The clast composition in the diamictite is consistently dominated by subangular, pale grey dolomite (grainstones and stromatolites) and black chert (Fig. 5d) (Hambrey, 1982; Harland *et al.*, 1993). Sandstone and siltstone clasts are less common and volcanic fragments have been reported (Fairchild & Hambrey, 1984) from a single region (measured sections 1–2). Harland *et al.* (1993) suggested that up to 10% of the clasts are striated, but probably the percentage is much lower, as neither dolomite nor chert clasts commonly preserve unequivocal striations. Rhythmites, interpreted by Hambrey (1982) as varvites, occur throughout the Petrovbreen Member and commonly contain fine dropstones. The lithological characteristics of the Petrovbreen Member suggest deposition in a glacimarine or glaciolacustrine setting (Hambrey, 1982; Fairchild & Hambrey, 1984; Harland *et al.*, 1993).

Figure 6 presents a $\delta^{13}C$–$\delta^{18}O$ cross plot of dolomite clasts, matrix, and varvites compared to carbonate samples from three sections of the Russøya Member in Spitsbergen. Although $\delta^{13}C$ of two of the clasts is negative, as is expected from the composition of the immediately underlying carbonates, most of the samples lie between 3‰ and 5‰. The carbon-isotopic compositions of these clasts are consistent with derivation from lower in the Russøya Member, as proposed by Fairchild & Hambrey (1984), but an Akademikerbreen source cannot be ruled out. Similarly, the chert clasts are most likely derived from the Russøya Member, where dark cherts commonly occur at the top of parasequences.

MacDonaldryggen Member

The MacDonaldryggen Member consists dominantly of terrigenous mudstone, but includes finely laminated carbonates < 1.0 m thick that occur directly above the Petrovbreen diamictite in several locations in Olav V Land [and were interpreted by Kaufman *et al.* (1997) as cap carbonates]. These carbonates are dark grey (tan weathering) limestones or dolomites in which wispy organic matter defines an anastomosing lamination (Harland *et al.*, 1993); they resemble the lean (< 40 cm) cap carbonate locally overlying the Gaskiers diamictite in Newfoundland (Myrow & Kaufman, 1998). However, $\delta^{13}C$ in the basal MacDonaldryggen carbonates (Fig. 7) is highly variable (-17‰ to 0‰) and in some cases clearly affected by the remineralization of organic matter (cf. Irwin *et al.*, 1977). This isotopic pattern (Fig. 7) is distinct from typical Neoproterozoic cap carbonates whose isotopic compositions are uniform globally (e.g. Hoffman & Schrag, 2002). Nor do these carbonates, which are in some cases interbedded with the underlying diamictite, mark an abrupt facies change as would be expected if they were deposited immediately following a Neoproterozoic glacial episode.

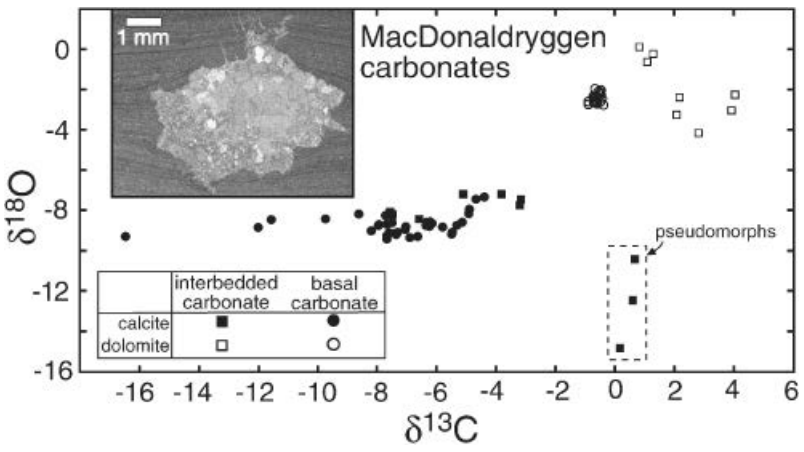

Fig. 7. $\delta^{13}C$–$\delta^{18}O$ cross-plot of base MacDonaldryggen carbonates, calcite pseudomorphs, and thin dolomite beds within the MacDonaldryggen Member shales. Note the extremely low $\delta^{13}C$ values for some of the calcite samples, which indicate that remineralized organic matter was a significant source of alkalinity (cf. Irwin *et al.*, 1977). Boxed data are from a sample at measured section 8 that contains the pseudomorph shown in the inset, interpreted here to be a glendonite nodule.

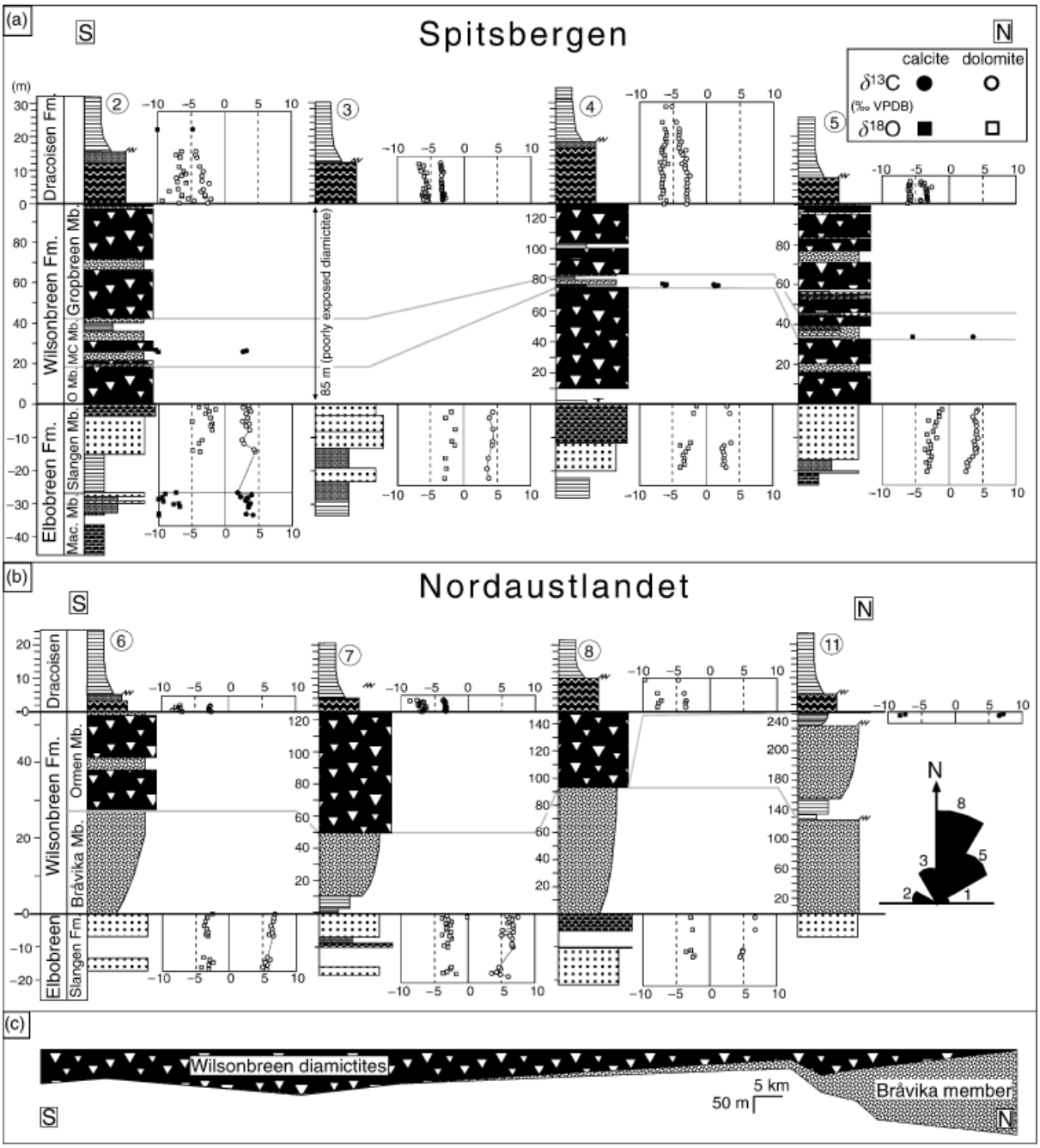

Fig. 8. Stratigraphic columns and isotopic data spanning the Wilsonbreen Formation in (a) northeastern Spitsbergen and (b) northwestern Nordaustlandet, with the top and bottom of the Wilsonbreen Formation as datums. Note the variable scale of the Wilsonbreen Formation and Bråvika Member. Grey lines in (a) show correlation of the Middle Carbonate in Member in Spitsbergen sections (absent in Nordaustlandet). Rose diagram shows palecourrent data ($n = 19$) for the Bråvika Member at measured sections 9–11. (c) Schematic cross-section (vertically exaggerated) of the Wilsonbreen diamictites and Bråvika Member, illustrating the northward thinning of the diamictites and reciprocal southward taper of the Bråvika sand wedge. See Fig. 4 for legend and the Supplementary material for tabulated $\delta^{18}O$ and $\delta^{13}C$ data.

The bulk of the MacDonaldryggen Member consists of finely laminated silty mudstone, dark olive green in colour. These uniformly fine-grained and parallel-laminated deposits are up to 200 m thick, contain minor sandy interbeds, and are virtually devoid of current-generated bedforms. At Slangen (measured section 2), the uppermost MacDonaldryggen mudstones grade upward into pure limestone ribbonites and grainstones with $\delta^{13}C$ values of 2–4‰ (Fig. 8). The top of the sequence here is an exposure surface, indicated by mudcracks within the limestones reported by Fairchild & Hambrey (1984), who also cite mudcracks in several other sections. However, most sections lack both carbonates and mudcracks, and the mudrocks instead pass gradationally into marly ribbonites of the lower Slangen Member.

The mudstone is speckled with rosette-shaped, calcite nodules, 2–10 mm in diameter (Fig. 7) that formed authigenically before the sediment was fully compacted. The nodules appear to be pseudomorphs of radial clusters of tightly nested crystals. They resemble glendonite pseudomorphs, which have long been used as a cold paleoclimate indicator (Boggs, 1972; Kemper & Schmitz, 1981; De Lurio & Frakes, 1999; Swainson & Hammond, 2001). The MacDonaldryggen pseudomorphs have not been studied in detail, but their external projections include both canted pyramidal and squared prismatic habits, which are diagnostic of the unusual crystal habit (Swainson & Hammond, 2001) of ikaite, monoclinic $CaCO_3 \cdot 6H_20$. Quaternary and modern ikaite tufa forms where waters rich in orthophosphate (a calcite and aragonite inhibitor) and Ca are discharged into alkaline waters that are close to their freezing point (Council & Bennet, 1993; Buchart *et al*., 1997). Authigenic ikaite crystals, precursor glendonites, have been found at shallow depths (2–8 m) in organic-rich sediments of the Antarctic shelf (Suess *et al*., 1982) and in estuaries of the southwest Beaufort Sea in Alaska (Kennedy *et al*., 1987). Most ancient glendonites are strongly depleted in ^{13}C (Boggs, 1972; Suess *et al*., 1982; De Lurio & Frakes, 1999), typically $-15‰$ to $-22‰$, and remineralized organic matter or anaerobically oxidized methane is widely cited as sources of the isotopically depleted carbonate. The MacDonaldryggen pseudomorphs are depleted in ^{13}C and ^{18}O, relative to dolomites forming discontinuous beds and concretions in the same mudrocks that are assumed to better represent seawater compositions (Fig. 7), but are not nearly as ^{13}C-depleted as typical glendonites. We emphasize that we have not studied the pseudomorphs in detail and that our interpretation that they are glendonites is tentative; the original mineral could have been gypsum or anhydrite, as is common in the Russøya Member (Fairchild & Hambrey, 1984).

Slangen Member

The Slangen Member (Fig. 8) is a regressive parasequence, 20–30 m thick, composed of silty to marly ribbons capped by pale grey, cherty dolomite. Much of the dolomite consists of cross-stratified grainstone, variably composed of ooids, tabular intraclasts and rounded dolomite grains (Fairchild & Hambrey, 1984; Harland *et al*., 1993). Tabular cross-bedding, well-defined by trains of bedding-parallel, chert-filled vugs (Harland *et al*., 1993), is common in the lower half of the grainstone. Dark microbialaminite occurs as thin lenses within the grainstone in some sections and as thicker deposits above the grainstone. The microbialaminite has a well-developed laminoid fenestrate fabric, with void-filling sparry calcite, length-slow chalcedony (Fairchild & Hambrey, 1984) and, in rare instances, either anhydrite or gypsum. The evidence for evaporite minerals and extremely high Na concentration in dolomite (2000–4000 p.p.m. at measured section 5) suggests that this unit was deposited in an intermittently restricted environment (Fairchild & Hambrey, 1984). The general facies and sequence are similar to those observed beneath the Recent coastal sabkhas (supratidal salt flats) of the southern Arabian Sea (e.g. Kendall & Skipwith, 1969), as discussed in detail in Fairchild & Hambrey (1984).

The upper contact of the Slangen Member typically is sharp, except at Ditlovtoppen (measured section 4), where the grainstone passes transitionally upwards into 2.5 m of mudcracked red siltstone with thin dolomite interbeds. Elsewhere, the top 5–20 cm below the contact is typically silicified and broken into angular and tabular clasts that show no evidence of reworking (Fairchild & Hambrey, 1984). Despite the evidence for exposure, no erosional or karstic relief is evident at the outcrop scale. Instead, the surface typically appears to be flat.

In Spitsbergen sections, $\delta^{13}C$ varies in the grainstone from 2.5‰ to 4.5‰ (Fig. 8a). In measured section 5, the section sampled in greatest detail, $\delta^{13}C$ rises smoothly through the grainstone by 2‰. $\delta^{18}O$ also increases by the same amount, lending credence to the interpretation that the grainstone was deposited in a progressively restricted environment. The Nordaustlandet sections (Fig. 8b) exhibit a similar pattern of $\sim$2‰ enrichment up section through the grainstone, but are on average 2–3‰ higher than the Spitsbergen sections (Fig. 9).

Spatially variable diagenesis on carbonate platforms commonly generates lateral difference in $\delta^{13}C$ of a similar or greater magnitude (e.g. Allan & Mathews, 1982; Chafetz *et al*., 1999) than those in the Slangen Member. However, the reproducibility of the upward positive $\delta^{13}C$ trend in all sections and deficiency in organic matter in the Slangen dolomites (Fairchild & Hambrey, 1984) suggest that the Slangen Member preserves a signal of evolving seawater $\delta^{13}C$. Insofar as this hypothesis is true, the $\delta^{13}C$ difference between Spitsbergen and Nordaustlandet sections may be interpreted in one of two ways: either it records a roughly north–south isotope gradient within the Svalbard basin, or the grainstone is diachronous within the Slangen Member, and in any given section captures only a portion of a longer term rise in marine $\delta^{13}C$ (Fig. 9). The former hypothesis implies a lateral isotope gradient of $\sim$2‰ (Fig. 9a), which is similar to $\delta^{13}C$ gradients between the inner and outer shelf in the Otavi Group of northern Namibia (Halverson *et al*., 2002) and is consistent with deposition of the grainstone in a restricted environment. On the other hand, simple stacking of the Nordaustlandet sections atop the Spitsbergen sections yields a nearly continuous $\delta^{13}C$ increase of 4‰ up section (Fig. 9b), consistent with progradation of the grainstone from south to north.

Wilsonbreen Formation

Bråvika Member

In Nordaustlandet and northernmost Ny Friesland (Heclahuken), a clean, medium-grained sandstone composed predominantly of well rounded quartz and chert grains separates the Slangen Member from the Wilsonbreen diamictites (Fig. 8). We informally refer to this unit as the Bråvika Member and include it within the Wilsonbreen Formation. The Bråvika Member thickens northward from

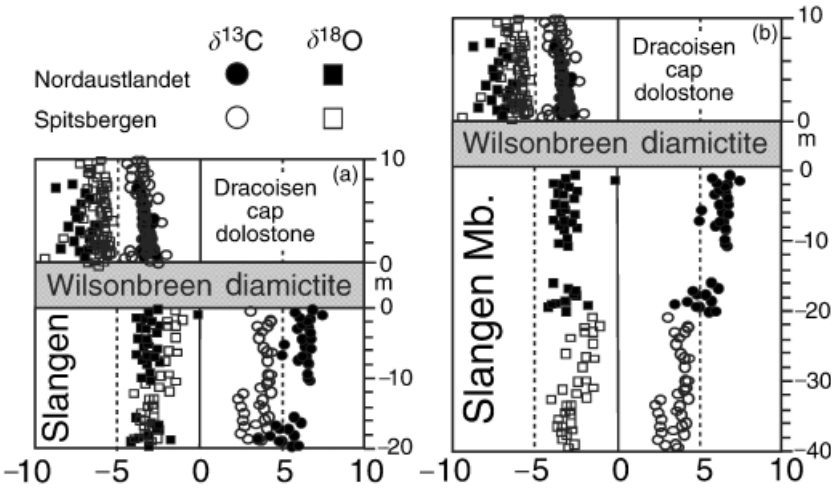

Fig. 9. $\delta^{13}C$ and $\delta^{18}O$ data from the Slangen grainstone (dolomite) and the Dracoisen cap dolostone, which bracket the Wilsonbreen Formation. Both intervals are scaled to a mean thickness. (a) If the grainstone was deposited everywhere synchronously, then the spread between the Spitsbergen and Nordaustlandet data indicate an $\sim$2‰ $\delta^{13}C$ gradient within the basin. (b) If the grainstone was deposited diachronously, such that it is younger to the north, the data indicate a gradual rise in $\delta^{13}C$ of 4‰ through the Slangen Member. In contrast to the variable isotopic values for the Slangen Member, both $\delta^{13}C$ and $\delta^{18}O$ through the Dracoisen cap dolostone are nearly identical in all sections, implying synchronous deposition throughout the basin, despite variations in thickness (3–18 m).

8 m at Ditlovtoppen (measured section 4) to 233 m at the north coast of Nordaustlandet (measured section 11). The Bråvika Member in measured sections 6–8 appears finer grained and recessive near the base, although the nature of the contact with the Slangen Member is obscured. Thin lenses of stromatolitic dolomite occur within the lower sandstones. In these locations, the top of the sandstone coarsens with the addition of angular dolomite clasts. The contact with the overlying diamictite is a sharp scour surface with a thin pebble lag, and the lower diamictites are rich in sand evidently reworked from the Bråvika Member.

In the northernmost exposure (measured section 11), the Bråvika Member comprises three distinct parasequences, a lower one dominated by sandstone (which we correlate with the entire Bråvika Member in measured sections 6–8), a middle one in which the sandstone contains angular, outsized, dolomite clasts, and an upper one composed of argillite and marly limestone ribbonites, capped by a 0.5-m-thick limestone-clast diamictite (beneath the basal Dracoisen cap dolostone). $\delta^{13}C$ in these carbonates $\approx$7‰, falling on the trajectory of increasing $\delta^{13}C$ defined by the Slangen Member (Fig 9b). Planar and trough cross-strata throughout measured section 11 indicate a mean paleoflow direction toward the north (Fig. 8), the direction of stratigraphic thickening.

The stratigraphic relations and geometry of the Bråvika Member (Fig. 8c) and overlying diamictite suggest that it is a diachronous unit, with sands being deposited in the northern part of the basin while Wilsonbreen diamictite was being deposited to the south. The coarsening upward nature of the sandstone sequence could reflect the approach of the Wilsonbreen ice sheet.

Diamictite

The Wilsonbreen Formation in Ny Friesland and Olav V Land (Fig. 8) is divided into three members (Harland *et al.*, 1993). The basal Ormen Member consists predominantly of poorly stratified diamictite with abundant lenses and interbeds of conglomerate, coarse sandstone, and breccia (Fairchild & Hambrey, 1984; Harland *et al.*, 1993). Clasts in the diamictite are dominantly carbonate, but sandstone, chert, gneiss and coarse-grained pink granite clasts also are abundant (Harland *et al.*, 1993). Striated and fractured stones are common (Harland *et al.*, 1993). The source of the metamorphic clasts is unknown. Ormen Member facies indicate deposition in a terrestrial setting, whereas the exotic clasts suggest deep erosion and glacial transport over long distances (Fairchild & Hambrey, 1984). Because glaciers were in contact with basement, carbonate and siliciclastic clasts in the diamictite could have been derived from any stratigraphic level in the sub-glacial succession.

The Middle Carbonate Member consists mostly of medium-grained, dolomitic sandstone, but is distinguished by thin carbonate beds found only in Ny Friesland and Olav V Land sections. On the Ormen nunatak (measured section 2), the carbonate is a 0.5-m-thick, silty, dolomitic microbial laminae. At Dracoisen (measured section 5), the carbonate occurs as multiple, thin ($<$0.1 m), discontinuous, and often scoured, isopachous limestone stromatolites encased within medium-grained sandstone. At Ditlovtoppen the carbonate occurs in 1.5 m of dolomite and limestone ribbonites and rhythmites. The $\delta^{13}C$ of all sampled carbonates, including those published by Fairchild *et al.* (1989), lie in a range of 1–5‰ (Fig. 8). Fairchild *et al.* (1989) argued that the carbonates were deposited in an evaporitic environment (during a period of glacial retreat; Fairchild & Hambrey, 1984) based on highly enriched $\delta^{18}O$ compositions (up to +10.8‰) of some dolomites, as well as the occurrence of gypsum casts and anhydrite relics in some samples. Whereas new analyses presented here yield much lower $\delta^{18}O$ values in limestone samples collected in

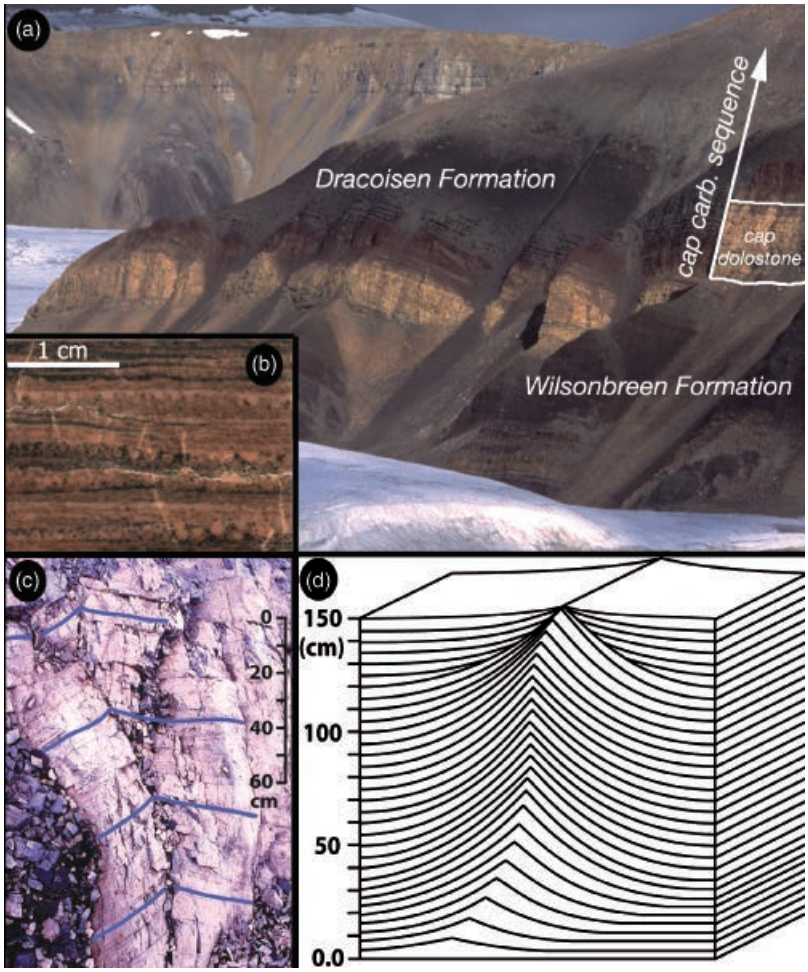

Fig. 10. (a) Field photograph of the upper Wilsonbreen Formation and overlying Dracoisen Formation at Ditlovtoppen (measured section 4), illustrating the uniform cap dolostone (18-m-thick), overlain by red, green, then black shales of the cap-carbonate sequence. (b) Polished slab slows low-angle cross-lamination, reverse-graded peloids, and black, interpeloid cement typical of the Dracoisen cap dolostone. (c) Field photograph with line work and (d) idealized sketch of typical megaripple structures, which exclusively occur in the upper half of the Dracoisen cap dolostone and other cap dolostones globally and demonstrate growth of the bedform by vertical accretion under oscillatory flow.

measured section 5 (Fig. 8a), high sulfate and Na (3500 p.p.m.; unpublished data) concentrations support the hypothesis that the Wilsonbreen carbonates formed in evaporitic waters, analogous to carbonate forming today in the Dry Valleys of Antarctica (Fairchild *et al.*, 1989), but with locally a large component of ^{18}O-depleted water, potentially derived from glacial runoff (Fairchild *et al.*, 1989).

The Gropbreen Member is variable in thickness and is similar lithologically to the Ormen Member, consisting mostly of poorly stratified, maroon diamictite (Fig. 10b). Clast composition is also similar, though with a greater proportion of basement material. A striated boulder pavement within Gropbreen diamictite at Ditlovtoppen has been reported (Chumakov, 1968, 1978), and sand wedge polygons occur in various sections (Chumakov, 1968, 1978; Harland *et al.*, 1993). At Gropfjellet, near Backlundtoppen, the sand wedges are developed in the uppermost diamictite layer and are filled by sand identical to that of an overlying, ripple cross-laminated sandstone.

On Nordaustlandet the diamictite is lithologically similar but has a higher concentration of volcanic clasts. Volcanic and granite clasts in Nordaustlandet are late Grenvillian in age (Johannson *et al.*, 2000), similar to the underlying basement (Gee *et al.*, 1995). The Middle Carbonate Member is absent on Nordaustlandet and the thickness of the diamictite is highly variable, reciprocating with the underlying Bråvika Member. These relations indicate that the diamictite on Nordaustlandet may be equivalent in age only to the Gropbreen Member in Ny Friesland, as would be expected from a northward advance of the Wilsonbreen ice front.

Dracoisen Formation (cap-carbonate sequence)

Like other Neoproterozoic caps worldwide (Williams, 1979; Aitken, 1991; Kennedy, 1996; Hoffman & Schrag, 2002), the Dracoisen cap dolostone (Fig. 10a) forms the transgressive base of a cap-carbonate sequence (cf. Hoffman & Schrag, 2002) that sharply overlies glacigenic diamictite without evidence of reworking or hiatus. Comparable in thickness to other cap dolostones (Williams, 1979; Hoffman & Schrag, 2002), the Dracoisen cap is thinnest (3 m) in Nordaustlandet (measured section 6) and thickest (18 m) at Ditlovtoppen in Ny Friesland (Fig. 10a). It weathers to a yellowish-tan colour and is a useful marker bed (Wilson and Harland, 1964). It is lithologically similar in all sections, composed of finely laminated,

micro- to macropeloidal dolostone with variable amounts of black, interpeloidal cement (Fairchild & Spiro, 1987). The peloids form discontinuous, normal- and reverse-graded laminae or overlapping pockets (Fig. 10b). The larger peloids are commonly truncated, flattened, or fused to one another, implying that they were not rigid particles (Fig. 10b). The preservation of such delicate structures attests to rapid cementation.

Very low-angle cross-stratification is common in the cap dolostone, particularly towards the top, where accretionary oscillation megaripples (Fig. 10c,d) also occur. The megaripples have characteristic wavelengths of 3–6 m and amplitudes of 20–40 cm with linear, parallel crests trending NW–SE (present-day), perpendicular to the inferred direction of trade winds. Individual sets of megaripples are up to 1.4 m thick.

The most complete section of the Dracoisen Formation (Fig. 11) is found at Ditlovtoppen (measured section 4) in southern Ny Friesland (Fairchild & Hambrey, 1984; Harland *et al.*, 1993). Here, the transgressive upper dolostone is transitional over a few meters through red siltstone and overlain by variegated red and green shales. Up section, the green shales pass into black shales, which comprise the remainder of the cap-carbonate sequence (Fig. 10a). Mud cracks mark the first evidence of subaerial exposure at 172 m above the base of the Dracoisen Formation. Above this level, the remainder of the Dracoisen consists mostly of mudcracked and ripple cross-laminated red and green siltstones with minor sandstone and interbedded dolomite beds, the most prominent of which is a 9-m-thick, microbialaminite dolomitic unit with cross-cutting cauliflower chert layers (Fairchild & Hambrey, 1984) ~230 m above the base of the Dracoisen Formation. No Ediacaran macrofossils occur in Svalbard, indicating a considerable hiatus (> 30 Myr) between the top of the Dracoisen and the overlying Tokammane Formation of Cambrian age (Knoll & Swett, 1987).

$\delta^{13}C$ and $\delta^{18}O$ data for the Dracoisen cap dolostone are plotted in Fig. 8. In all sampled sections, $\delta^{13}C$ begins at ~ -3‰ at the base and gradually decreases by about 1‰ through the dolostone. This trend is consistent throughout northeastern Svalbard, as seen in Fig. 9, in which a composite plot of all data, normalized to a constant cap dolostone thickness, show variation of less than ~1‰. Locally (e.g. measured section 4) carbonate interbeds occur above the cap dolostone, and $\delta^{13}C$ in these records a continued decline to a low of -5‰. $\delta^{18}O$ also exhibits a rough negative trend through the dolostone, falling about 1‰ from a low of ~ -5‰ at the base. These values are lower on average by ~4‰ than typical dolomites in Svalbard, but typical of other Neoproterozoic cap dolostones (Halverson, 2003).

Sparse carbonate beds in the middle and upper Dracoisen record a pronounced rise in $\delta^{13}C$ to highly enriched

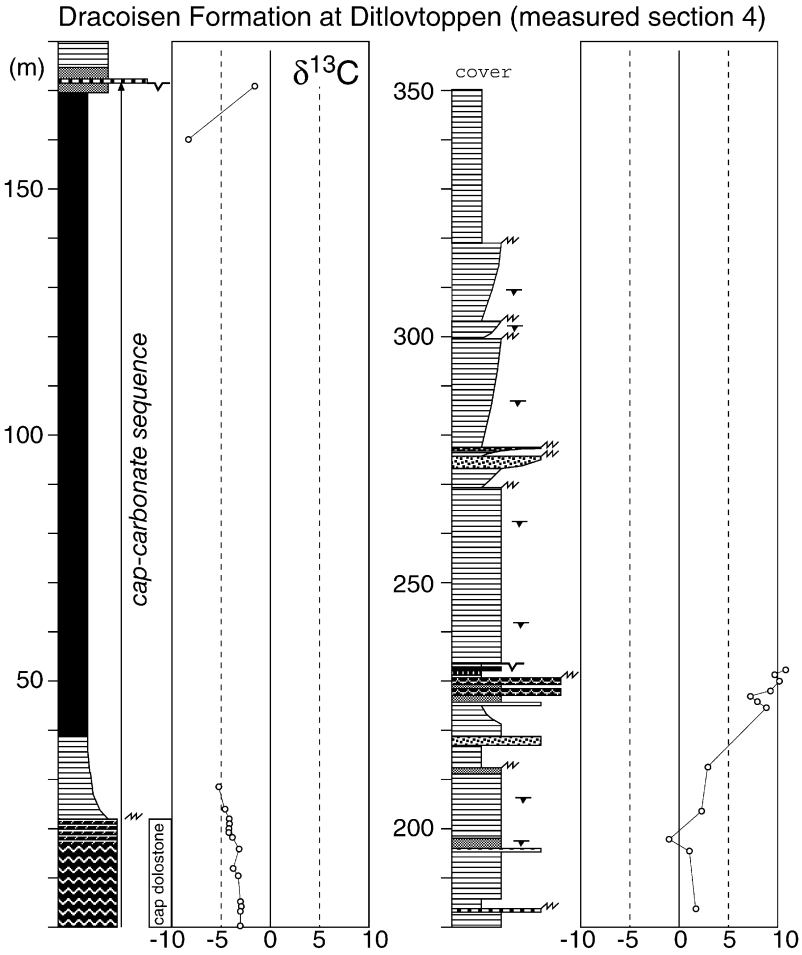

Fig. 11. Stratigraphic and $\delta^{13}C$ profile for the Dracoisen Formation at Ditlovtoppen (measured section 4). See Fig. 4 for the legend and the Supplementary material for tabulated data.

values ($> +10$‰) in the dolomite beds in the middle of the Formation. This rise coincides with sedimentary features (mud cracks and evaporates) that suggest at least intermittent restriction of the basin, and therefore, may not represent the evolution of open marine $\delta^{13}C$.

Elemental chemistry of the Dracoisen cap dolostone

Elemental data from three sections of the Dracoisen cap are summarized in Fig. 12. The relative ^{18}O-depletion, very high concentration of Fe and Mn, and high Mn/Sr of the Dracoisen cap are characteristic of digenetic alteration by meteoric fluids (Brand & Veizer, 1980, 1981; Banner & Hanson, 1990; Jacobsen & Kaufman, 1999). However, stratigraphic and geochemical characteristics are inconsistent with extensive meteoric diagenesis. First, the cap dolostone is bounded above by a flooding surface with no evidence for exposure, and therefore, it seems unlikely that it was subjected to extensive meteoric fluid flow after deposition. Second, the meteoric diagenesis model (Banner & Hanson, 1990; Jacobsen & Kaufman, 1999) predicts that given the very high Mn/Sr ratios in the dolomites (10–40 mol mol^{-1}), both $\delta^{13}C$ and $\delta^{18}O$ should have equilibrated with the meteoric fluids (Banner & Hanson, 1990). The strong reproducibility in $\delta^{13}C$ and the preservation of a distinct trend in all sections contradicts this model. Second, the high Na concentrations (1200–3800 p.p.m.) is the opposite of what one would predict had the cap dolostone seen a large flux of fresh water, and would seem to indicate that if the dolostone was diagenetically altered, it would have been under restricted, hypersaline conditions, for which there is no other evidence. Therefore, we regard the unusual geochemistry of the Dracoisen cap dolostone not as a record of pervasive alteration, but as a manifestation of the unusual hydrological and geochemical conditions in the aftermath of glaciation (Hoffman *et al.*, 2002).

DISCUSSION

The Pre-Petrovbreen $\delta^{13}C$ anomaly

The most salient feature in the isotopic compilation through the Polarisbreen Group is the large negative anomaly ($\sim$11‰) in the upper Russøya Member, just beneath the Petrovbreen diamictite. $\delta^{13}C$ declines smoothly through shallow-water sediments in Nordaustlandet sections, which rules out a huge depth-dependent isotope gradient (cf. Shields *et al.*, 1997; Calver, 2000; Fairchild *et al.*, 2000) as the source of the anomaly. Furthermore, in order for the full isotopic decline to have been recorded in shallow-water carbonates, it must have preceded any rapid sea-level drawdown related to the buildup of continental glaciers. This buildup of glaciers would have lowered sea level and exposed the Polarisbreen platform to erosion prior to deposition of the Petrovbreen diamictite. We interpret the absence of the anomaly in measured sections 3 and 5 as a consequence of this pre-glacial erosion and note that the thickness of the Petrovbreen diamictite in each section broadly coincides with the apparent depth of erosion, as inferred from the extent of truncation of the $\delta^{13}C$ anomaly

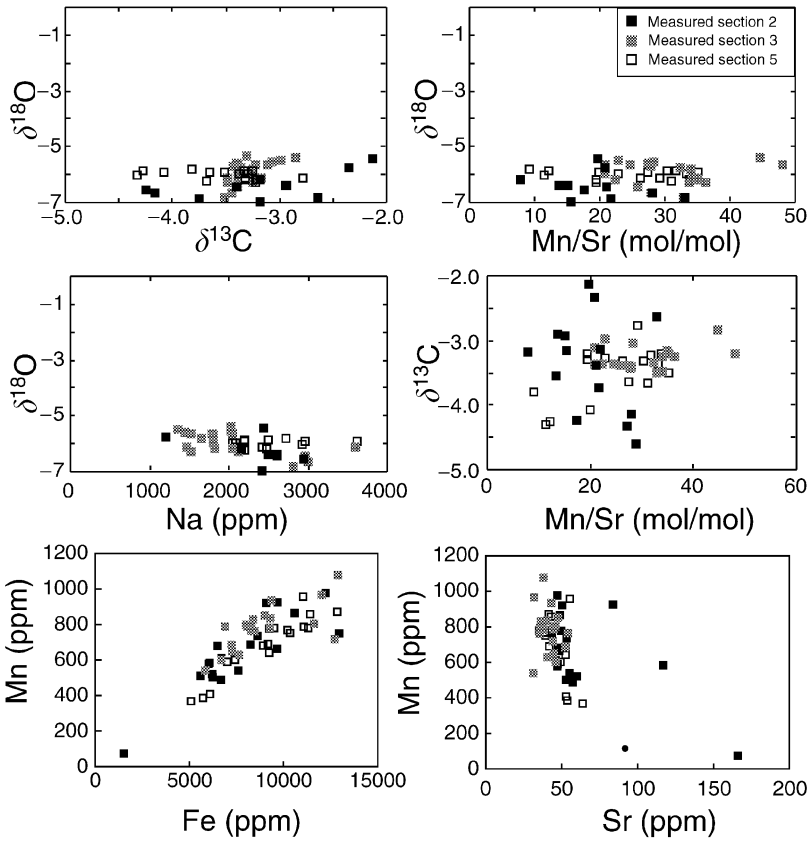

Fig. 12. Isotopic and elemental cross-plots for three sections of the Dracoisen cap dolostone.

(Fig. 4). The truncation of the upper Russøya Member is variable, and, along with the preservation of isotopically negative clasts in the Petrovbreen, rules out the possibility that the anomaly was the result of extreme diagenetic overprinting beneath the Petrovbreen exposure surface (Halverson *et al.*, 2002).

The stratigraphic constraints on the pre-glacial $\delta^{13}C$ anomaly are homologous to those for a pre-glacial anomaly of identical magnitude in the upper Ombaatjie Formation (Otavi Group), beneath the Marinoan-aged Ghaub glacial deposits in northern Namibia (Halverson *et al.*, 2002) (Fig. 13). In both cases, stratigraphic evidence indicates that the full negative shift occurred prior to the onset of continental glaciation, thus removing glaciation as a possible cause for the anomaly. Similar pre-glacial negative $\delta^{13}C$ anomalies (Fig. 13) occur globally, including in the Mackenzie Mountains in northwest Canada (Keele Formation; Hoffman & Schrag, 2002), the Adelaide Rift Complex, South Australia (Enorama and Trezona Formations; Walter *et al.*, 2000; McKirdy *et al.*, 2001), and Scotland (Lossit Formation, Brasier & Shields, 2000). In all cases, the decline appears gradual, punctuates trends of enriched composition ($> 5‰$), and is followed by a trend towards more positive values directly beneath the overlying glacial deposits. In Namibia, Canada, and Australia, the anomalies precede the younger of two discrete glaciations (Fig. 13), and no comparable anomaly is known from beneath the older, Sturtian, glaciation. In these three successions, the Sturtian glacial deposits host significant volumes of banded iron formation and are overlain by organic-rich cap-carbonate sequences with similar carbon-isotopic signatures (Kennedy *et al.*, 1998; Hoffman & Schrag, 2002). Likewise, the cap-carbonate sequences to the younger, Marinoan, glaciations in these three areas are similar to one another stratigraphically, sedimentologically, and isotopically (Hoffman & Schrag, 2002). We assume that the older and younger glaciations in Namibia, Canada and Australia were coeval (Kennedy *et al.*, 1998). Since pre-glacial negative $\delta^{13}C$ anomalies occur only beneath the Marinoan glacial deposits, we propose that this anomaly is a useful global correlation tool that can be used where obvious Sturtian–Marinoan glacial pairs are absent.

The Marinoan cap carbonate

The sedimentary record of deglaciation is contained in the transgressive Marinoan cap-carbonate sequence worldwide (Kennedy *et al.*, 1998; Hoffman & Schrag, 2002). Comparative studies have shown the Marinaon cap carbonates to be lithologically variable, with particular facies-specific structures and textures, including megaripples, peloids and seafloor-encrusting cements (Aitken, 1991; Grotzinger & Knoll, 1995; Kennedy, 1996; James *et al.*, 2001; Hoffman & Schrag, 2002; Nogueira *et al.*, 2003). The most widespread feature of these sequences is the basal cap dolostone, which is typically 3–20 m-thick and consists of pale yellow to grey, finely laminated, flinty dolomite (Hoffman & Schrag, 2002), bounded above by a flooding surface. Megaripples, which we interpret to reflect rapid deposition on a severe, storm-dominated shelf, are characteristic of most cap dolostones and consistently occur in the upper part of the unit. The homology of the Dracoisen cap dolostone and the Ravensthroat cap dolostone in northwest Canada (Fig. 13) is particularly striking, but virtually all of the distinctive features observed in the Dracoisen cap dolostone are shared by other cap dolostones in outer shelf settings in Australia (Kennedy, 1996), Namibia (Hoffman, 2002) and South America (Nogueira *et al.*, 2003) as well. Moreover, the carbon isotope profile through the Dracoisen cap dolostone is indistinguishable from other Marinoan cap dolostones (Fig. 13).

The Polarisbreen glaciation

Unlike Namibia, Canada and Australia, the pre-glacial carbon-isotope anomaly in Svalbard precedes the older of the two diamictite-dominated units. If the Petrovbreen and Wilsonbreen Formations are regarded as separate glaciations (Hambrey, 1982; Fairchild & Hambrey, 1984; 1995; Kennedy, 1998), then correlation of the Russøya anomaly with the overseas successions (Fig. 13) implies that the Petrovbreen is Marinoan and the Wilsonbreen represents a third, post-Marinoan, glaciation (Hoffman & Schrag, 2002). However, this interpretation is difficult to reconcile with the striking similarity of the Dracoisen cap dolostone with Marinoan caps elsewhere, and with the absence of any cap carbonate on top of the Petrovbreen diamictites. These correlation problems disappear if the Petrovbreen and Wilsonbreen diamictites, along with the intervening interval, encompass a single glacial episode equivalent to the Marinoan. For simplicity, we call this the Polarisbreen glaciation. If we are to accept the evidence from elsewhere that the Marinoan was a snowball Earth episode (Hoffman & Schrag, 2002), then the sedimentary succession representing the Polarisbreen glaciation must also be compatible with the snowball hypothesis.

In the paragraphs that follow, we use stratigraphic information from East Svalbard (given above) and East Greenland (from the literature) to develop a possible scenario (Fig. 14) in which the entire succession from the base of the Petrovbreen diamictites up through the Dracoisen cap dolostone (Ulvesø Formation through Canyon cap dolostone in East Greenland; Fig. 1) is accounted for as phases of a single, snowball-type, climatic cycle. We propose that the older and younger diamictites record the creation (Fig. 14, Phase a) and destruction (Fig 14, Phase d) of the snowball conditions, but that the fully established snowball episode – defined as having thick (> 100 m) sea ice covering the open ocean globally (Warren *et al.*, 2002) – is represented by the fine clastics of the MacDonaldryggen Formation (Fig. 14, Phase b) and the regressive carbonate-evaporite sequence of the Slangen Member (Fig. 14, Phase c). Although our paleoclimatic interpretation of the overall succession is unconventional in several respects, we believe it is consistent with (1) our field observations and

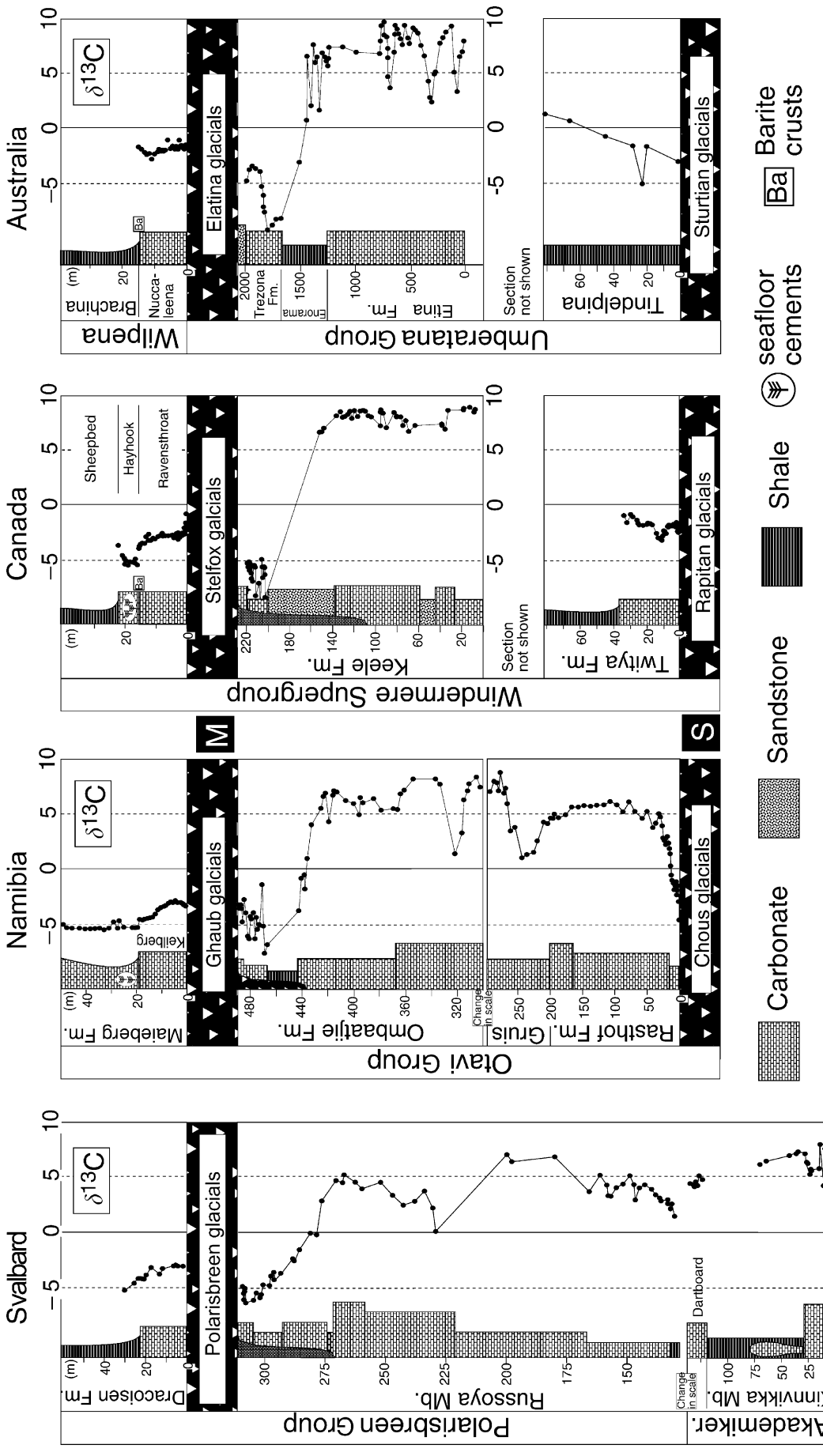

Fig. 13. Comparison of the composite $\delta^{13}C$ profiles spanning the Polarisbreen glaciation in Svalbard with profiles spanning glaciations of presumed Sturtian (labelled 'S') and Marinoan ('M') age in northern Namibia, northwest Canada, and South Australia. The cap dolostones and pre-Marinoan $\delta^{13}C$ anomalies are homologous in all four successions and are the bases for assigning both Polarisbreen diamictites to the Marinoan ice age. Evidence of Sturtian glaciation in Svalbard is absent, but we argue that the lower Russøya Member (base Elbobreen Formation) represents the Sturtian cap carbonate on the EGES platform. Note that portions of the Canada and Australia profiles are omitted due to absence of $\delta^{13}C$ data. The Namibia, Canada, and Australia profiles are modified from Hoffman & Schrag (2002).

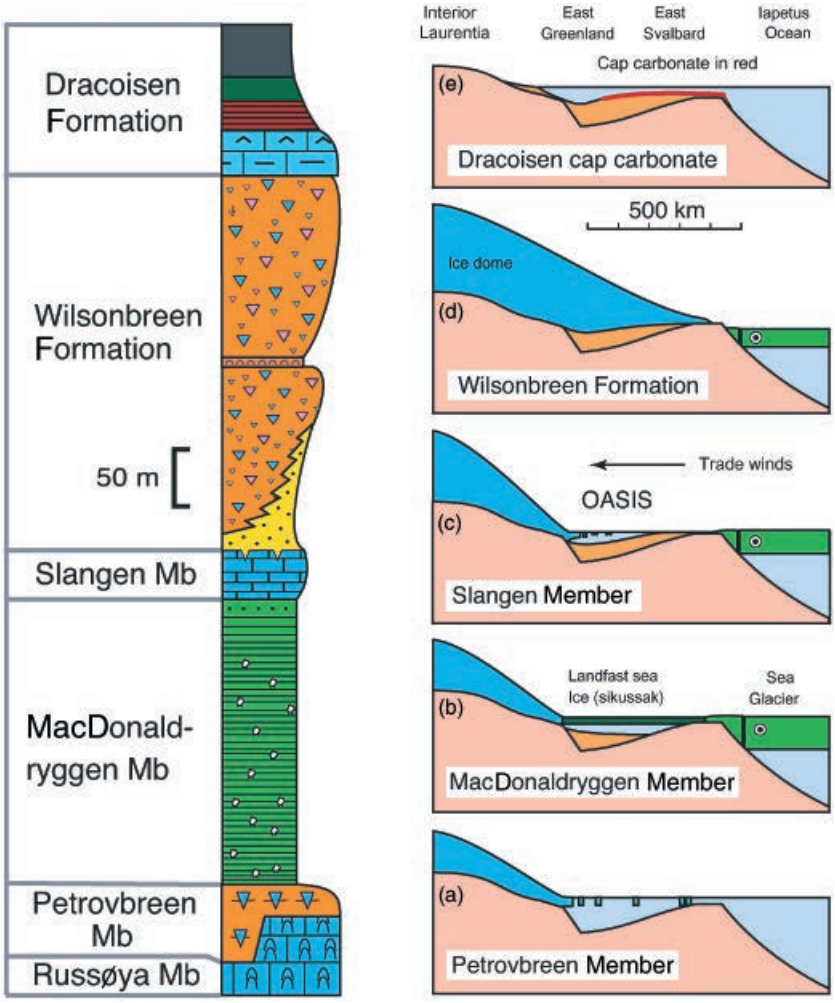

Fig. 14. The Marinoan glaciation in east Svalbard and East Greenland, interpreted in terms of a five-phase (a–e) snowball-type climatic cycle. The cross-section is drawn along a north-south line (in present coordinates) across the EGES platform. Formation/Member names are derived from Spitsbergen (Fig. 1). The stratigraphic section to the left (scaled to thickness) is a schematic version of that developed in the text and figure Fig. 3 and is plotted to correspond to the cross sections on the right. Phase (a): An ice dome advanced over the coastal highlands of Laurentia/East Greenland, heralding the onset of local glaciation prior to full snowball conditions. The advancing ice led to deposition of Petrovbreen Member glacimarine diamictites above a karstic erosional surface within the stromatolitic Upper Russøya Member. Phase (b): Full snowball conditions were marked by MacDonaldryggen Member mudstones, which were deposited beneath sikussak ice by sediment laden, subglacially derived, meltwater plumes. Pseudomorphs are abundant in the mudstone, and the top of the unit in more glacioproximal East Greenland sections often contains dropstones related to the breakup of the sikussak ice. Phase (c): As equatorial temperatures rose, the sikussak ice disintegrated over the EGES platform. However, sea glaciers were still fed by ice flow from polar latitudes, therefore an oasis of open ocean developed on the EGES platform while ice still covered much of the world's oceans. Trade winds would have fed the ice dome with moisture from the oasis and kept glacially derived icebergs and winter sea ice stacked along the East Greenland side of the platform. Dolomite grainstones of the Slangen Member were deposited on the East Svalbard side of the platform. Phase (d): Reinvigoration of the hydrologic cycle due to the opening of snowball oases on tropical shelves led to the growth of ice domes. Bråvika Member sandstones were reworked into glaciofluvial outwash and eventually overridden by the advancing ice. Terrestrial diamictites and glaciolacustrine carbonates of the Wilsonbreen Fm were deposited proximal to the ice dome. Phase (e): The basal Dracoisen Fm cap dolostone was deposited in the immediate aftermath of the snowball Earth, when tropical temperatures finally reached levels sufficient to melt the sea glacier. The cap dolostone is not preserved in the deepest part of the platform. See the Discussion section of the text for a full explanation of each phase.

isotope data, (2) previously published isotopic data, (3) our proposed inter-regional correlation criteria and (4) recent theoretical advances in the glacial dynamics of snowball Earth (Warren *et al.*, 2002; Donnadieu *et al.*, 2003; Goodman & Pierrehumbert, 2003).

Phase a: Petrovbreen Member (Ulvesø Formation): buildup of subtropical ice domes

The first physical sign on the EGES platform of the coming ice age was a ~50-m sea level drop related to the

growth of high latitude and high altitude glaciers. Semi-arid conditions prevailed on the exposed EGES platform, where tens of meters of karstic relief developed (Fig. 4). Trade winds deposited aeolian sandstones preserved in the present-day northwest portion of the platform (Hambrey & Spencer, 1987; Moncrieff and Hambrey, 1990). As the subtropics cooled, moisture delivered from the open ocean (in the present-day east) began to accumulate as ice in paleo-highlands now situated in the hinterland of southern East Greenland (Higgins *et al.*, 2001). An ice dome nucleated in these highlands (Moncrieff, 1989; Phillips & Fredricksen, 1981; Henriksen, 1981; Smith & Robertson, 1999b) and descended to sea level (Fig. 14a), depressing the EGES platform glacioisostatically. Massive diamictites as thick as 300 m (Ulvesø Formation) accumulated at the grounding line of the ice sheet in the southwestern part of the platform (Higgins, 1981; Hambrey & Spencer, 1987), while ice-rafted debris rained-out over present-day northern and eastern regions (Fairchild & Hambrey, 1984; Hambrey & Spencer, 1987; Harland *et al.*, 1993), filling topography and leaving a thin veneer of glacimarine diamictite (Petrovbreen Formation).

Clasts in the Petrovbreen diamictites are subrounded to subangular (Fig. 5d), suggesting that they were transported at least partially as subglacial debris and that sources of angular englacial debris such as nunataks were not important (Dowdeswell *et al.*, 1985; Hambrey & Spencer, 1987, and references therein). Clasts were derived entirely from the directly underlying sedimentary units indicating that the ice sheet was likely cold-based and unable to accomplish extensive bedrock quarrying (Cuffey *et al.*, 2000; Atkins *et al.*, 2002). The abundance of dropstones in distally deposited glacimarine sediments also points to a cold-based ice sheet with little or no ice shelf (< 70 km wide) that was capable of calving cold, debris-rich icebergs (Carey & Ahmed, 1961; Orheim & Elverhoi, 1981). Together, these observations indicate that by the end of Petrovbreen/Ulvesø times, the platform was dominated by a cold-based ice dome that was grounded in the present-day southwest of the platform and which distributed debris-rich icebergs to the rest of the platform. At least two sand wedge horizons in the Ulvesø Formation (Spencer, 1985; Hambrey & Spencer, 1987; Moncrieff & Hambrey, 1990), indicative of subaerial exposure and thermal contraction cracking of permafrost, imply a fluctuating ice line that left some regions of the western platform intermittently ice-free.

Phase b: MacDonaldryggen Member (Arena Formation): formation of sikussak ice

Across the entire EGES platform, glacimarine diamictites terminate abruptly at the top of the Petrovbreen/Ulvesø Formation (Hambrey & Spencer, 1987; Harland *et al.*, 1993). The succeeding MacDonaldryggen/Arena Formation consists of dropstone-free, finely laminated, silty claystone and fine sandstone. In the grounding-line-proximal regions of SW East Greenland, the Arena Formation is significantly coarser and contains two distinctive dropstone horizons indicating that some form of glaciation persisted. More distal sections in NE Svalbard consist of thick, finely laminated deposits that lack current-generated bedforms, but are speckled with glendonite nodules. We propose that the abrupt termination of ice-rafted debris at the top of the Petrovbreen/Ulvesø Formation does not mark the end of a glaciation, but rather the abrupt transition into a snowball Earth (Hoffman & Schrag, 2002). How do we rationalize this interpretation? We must first step back and consider some basic features of ice dynamics and their probable role in the development and maintenance of a snowball Earth.

Theory suggests that ice dynamics play a critical role in the advance of sea ice to the Equator (Warren *et al.*, 2002; Goodman & Pierrehumbert, 2003; Lewis *et al.*, 2003). In simulations lacking ice dynamics, vertical mixing at the ice lines halts the advance of sea ice, preventing a snowball Earth (Poulsen *et al.*, 2001; Poulsen, 2003). The dynamics of sea ice hasten the ice-line advance by transporting latent heat poleward and fresh water equatorward. The physical mechanisms are varied, from dispersal of drift ice by winds and currents (Lewis *et al.*, 2003), to gravitational flowage of thick (> 100 m) sea ice toward the zone of melting (Goodman & Pierrehumbert, 2003). The latter phenomenon is aptly described as a 'sea glacier' (Warren *et al.*, 2002). Goodman & Pierrehumbert (2003) find that at dynamic steady state, a sea glacier poised at the brink of ice-albedo runaway would be $\sim$0.2-km thick in polar and middle latitudes, but would taper to zero thickness at the 0 °C isotherm. Ice flow velocities peak at 2 km yr^{-1} near the ice edge and result in the deposition there of the meltwater equivalent of 1.5 m of additional precipitation annually (Goodman & Pierrehumbert, 2003). This freshwater input not only raises the freezing point, but also suppresses vertical mixing at the ice line.

Simulations with ice dynamics revive the classic concept of ice-albedo instability, wherein the final invasion of sea glaciers through the tropics occurs rapidly ($\sim$1.6 kyr if melting ceased) due to runaway ice-albedo feedback, after which the ice slowly thickens for a few thousand years as the ocean loses its reservoir of solar heat (Warren *et al.*, 2002). Once the ice fronts meet at the equator, maximum ice flow velocities slow to just 55 m yr^{-1} in the simulation (Goodman & Pierrehumbert, 2003), but this inflow rate maintains $\sim$0.45 km of ice at the equator (vs. 0.2 km for static ice) and reduces ice thickness in the middle and polar latitudes to $\sim$1.0 km (vs. 2 km at the poles in the static case). Equatorward flowage of the sea glacier is balanced by poleward vapor transport and by melting and freezing at the base of the ice in the tropics and extratropics, respectively.

If a snowball glaciation took place, the synglacial sedimentary record on continental margins should reflect the dynamic interplay between three types of ice mass (Fig. 14): (1) the mobile sea glacier, (2) shorefast, multi-annual, sea ice (known as *sikussak*; Koch, 1945) on continental shelves, shallow platforms and inland seas and (3) terrestrial glaciers and ice domes. Given the proximally deepened bathymetric profile characteristic of glaciated

shelves (Anderson, 1999), we may expect the shear zone between the sea glacier and the shorefast sikussak to occur at the outer edge of the shelf (Fig. 14b). The maximum thickness of sikussak ice, given adequate water depth, should approximate that of 'static' ice in the simulations described above. In reality, sikussak ice will be thinner due to subglacial meltwater runoff from adjacent ice domes, analogous to the thin ice on the present Antarctic Dry Valley lakes (e.g. McKay *et al*., 1985). At middle and high latitudes, sikussak ice will be thicker than the adjacent sea glacier and will readily become entrained in the glacial flow. In the subtropics and tropics, however, sikussak ice will be thinner than the bounding sea glacier, which will tend to encroach onto the shelf and buttress the shorefast sikussak. Counterintuitively then, abrupt invasion of sea glaciers into the tropics would have the effect of blocking the flow of terrestrial glacier ice onto the platform (Fig. 14a, b). With the platform covered by sikussak ice, the terrestrial ice sheet could no longer calve and the source of dropstones would be removed (Funder *et al*., 1998; Dowdeswell *et al*., 2000). Thus, the abrupt termination of the Petrovbreen/Ulvesø diamictites and associated ice-rafted debris need not signify the end of the glaciation. But is the MacDonaldryggen–Arena Formation compatible with sedimentary processes active on the platform during a snowball glaciation?

The sea glacier and shorefast sikussak would backstop tidewater glacial flow (Fig. 14b), causing the terrestrial ice sheet to slowly thicken (De Angelis & Skvarca, 2003), despite the severe reduction in precipitation rate when the ocean is frozen. Net sublimation at the sea surface in the subtropics would provide moisture borne by trades that would precipitate as ice in the coastal highlands bordering the platform (Fig. 14b). Numerical simulations by Donnadieu *et al*. (2003) imply that a dynamic polythermal ice sheet could develop in as little as 180 kyr after snowball onset from sublimation-derived moisture alone. If the ice dome became even partially warm-based, ice loss would have been accommodated by subglacial meltwater streams rather than calving, and basal melting at the grounding line would have rendered shelf-ce free of debris, further reducing the chance of generating ice-rafted debris basinward of the grounding line (Carey & Ahmed, 1961; Drewry & Cooper, 1981; Orheim & Elverhoi, 1981; Alley *et al*., 1989). Net evaporative mass loss from the surface of the sikussak would have caused diffusive cooling through the ice column and freezing of seawater to its base. Persistent upward advection of sikussak ice would have prevented any wind-blown, glacier-derived, or anchor ice-derived (Reimnitz *et al*., 1987) debris from raining out as ice-rafted debris. The notable absence of ice-rafted debris in the MacDonaldryggen/Arena laminites distant from the grounding line is compatible with a frozen ocean.

Sublimation at the surface of the sikussak would cause freezing of sea water at its base, generating dense brines that would sink to the bottom and flow basinward as density currents. When amplified by tidal pumping, density currents may reach velocities high enough to transport sand and cut sinuous channels 40 m deep (Elverhøi *et al*., 1989; Dowdeswell *et al*., 1998). During the Pleistocene, laminated facies in Antarctica (Orheim & Elverhøi, 1981) and Greenland (Dowdeswell *et al*., 1998) are restricted to interglacial periods when open water is available for sea ice formation, and the resulting brine-driven traction currents are able to deliver coarse sediment to distal, otherwise shale-dominated regions. On the Barents shelf today, brine-driven gravity currents formed during sea ice formation account for as much as 70% of the annual sedimentation in distal environments (1.4–3.5 cm kyr^{-1}), the other 30% coming mostly from ice-rafted debris entrained in sea ice delivered from the Russian Arctic and subordinately from the edges of buoyant, subglacially derived meltwater plumes (Elverhøi *et al*., 1989). The scouring, winnowing and rippling visible in grounding-line proximal sands of the Arena Formation (Hambrey & Spencer, 1987) are consistent with brine-driven density currents generated by freezing seawater at the base of the sikussak in response to surface sublimation.

Phase c: Slangen Member: sikussak melts away and a snowball oasis appears

Atmospheric CO_2 concentrations and greenhouse forcing must slowly rise on a snowball Earth because silicate weathering cannot balance volcanic outgassing. After millions of years (Caldeira & Kasting, 1992), tropical sea-surface temperatures reach 0 °C and sea ice begins to melt. Whereas the stagnant sikussak could melt off completely, creating an oasis of open water on the EGES platform (Fig. 14c), the tropical ocean would remain sealed off because of glacial inflow from middle and high latitudes (Goodman & Pierrehumbert, 2003). We propose that the upper part of the MacDonaldryggen/Arena Formation and the Slangen regressive carbonate-evaporite sequence (Fig. 8) were deposited in a snowball oasis over the EGES platform. Carbonate sediment was produced under evaporative conditions in the oasis and quickly prograded to form a vast supratidal sabkha as base level fell. The existence of extensive open water and warmer temperatures would have intensified vapor transport and snow accumulation on downwind ice domes. Expansion of these and other ice sheets globally would have caused glacioeustatic lowering, consistent with seaward (northward) progradation and subaerial exposure (offlap) of the Slangen carbonate bank. Weathering of carbonate detritus of glacial origin could provide the alkalinity flux necessary to precipitate new carbonate within the basin (Fairchild *et al*., 1989).

Kennedy *et al*. (2001) reported high $\delta^{13}C$ compositions from purportedly syn-glacial (Marinoan) carbonates and interpreted them to demonstrate relatively high fractional burial of organic matter during the glaciation. Whereas our interpretation of the ^{13}C-enriched Slangen Member as syn-glacial is consistent with their findings, its isotopic composition may reflect other factors, including the $\delta^{13}C$ of the carbonate available for weathering during the glaciation (Higgins & Schrag, 2003). Additionally, the limited

dissolved organic carbon reservoir in the oasis would be dominated by the huge atmospheric reservoir (0.1–0.2 bar CO_2; Caldeira & Kasting, 1992). The latter would not be isotopically equilibrated with the ocean, but instead with volcanic input with $\delta^{13}C \approx -5‰$ to $-7‰$ (Des Marais & Moore, 1984). Consequently, the $\sim -13‰$ equilibrium fractionation between CO_2 and calcite for seawater at 0 °C (Friedman & O'Neil, 1977) could result in carbonate being precipitated in the oasis with $\delta^{13}C$ as heavy as 6–8‰ (Higgins & Schrag, 2003), irrespective of any contribution from carbonate dissolution or organic matter burial. The rapid rise in $\delta^{13}C$ observed in the Slangen carbonates could reflect equilibration with the mantle-dominated atmospheric carbon reservoir.

On the landward part of the platform, no equivalent to the Slangen Member is preserved. Glacial erosion and glacioisostatic loading had probably created a landward-dipping inner shelf region (consistent with SW-directed paleocurrents in upper Arena Formation and younger units of East Greenland; Hambrey & Spencer, 1987), where deeper waters were maintained and where onshore winds tended to stack seasonal sea ice and icebergs (Fig. 14c). The uppermost Arena Formation contains a sudden reappearance of ice-rafted debris, including boulder-sized granite dropstones (Moncrieff & Hambrey, 1988) that may reflect the final disintegration of the local sikussak, mobilizing outlet glaciers from the inland ice dome. The presence of granite clasts indicates that ice streams had eroded down to basement in the hinterland.

Phase d: Wilsonbreen Fm: inland ice dome advances onto a sand sea

Increased precipitation in the hinterland caused the ice dome to expand and flow more actively. The ice margin advanced across the EGES platform (Fig. 14c, d), creating a grooved and striated peneplane (Moncreiff & Hambrey, 1988) on which polymictic diamictites and sandstones of the Wilsonbreen/Storeelv Formation were deposited. Subglacial channel sands and tills (containing abundant metamorphic basement clasts) indicate that the ice sheet was at least partly warm-based (Chumakov, 1968; Dowdeswell, 1985; Harland *et al*., 1993). Sands that had collected on the exposed Slangen bank were reworked by northward-flowing proglacial streams. These deposits (Bråvika Member of the Wilsonbreen Formation) thicken northward at the expense of the diamictites (Fig. 8c), and coarsen upward related to the approach of the glacier terminus (Fig. 14d). Sand wedges indicative of subaerial exposure are developed on various horizons within the Wilsonbreen (Chumakov, 1968; Harland *et al*., 1993) and Storeelv (Spencer, 1985; Hambrey & Spencer, 1987; Moncrieff, 1990) diamictites. Thin carbonate horizons in the middle Wilsonbreen Formation of southern East Svalbard (Fig. 9) precipitated in evaporative, dry-valley lakes fed by glacial meltwater (Fairchild & Spiro, 1987; Fairchild *et al*., 1989).

As with the initial Petrovbreen/Ulvesø glaciation, the hinterland ice front on the EGES platform was unstable during the terminal Wilsonbreen/Storeelv reglaciation. Orbital forcing, sea-ice switching (Gildor & Tziperman, 2000), binge-purge cycling (MacAyeal, 1993), ice-stream migration (Payne & Donglemans, 1997), or a host of other factors could account for the observed instability. Even small changes in glacial mass balance or local base level could dramatically change the paleogeography of the platform. As greenhouse forcing continued to rise, the hinterland ice sheet ultimately expanded close to the present northern exposed limits of the platform.

Phase e: Dracoisen cap dolostone: sea glaciers collapse and cataclysmic deglaciation ensues

With CO_2 levels continuously rising, the melting rate of the tropical sea glacier eventually overtook the inflow rate of ice from higher latitudes. The equatorial ice rapidly thinned and open water appeared, greatly intensifying the reverse ice-albedo and water-vapor greenhouse feedbacks. The sea glacier quickly collapsed, melting away in a period of $\sim$100 yrs (R.T. Pierrehumbert, pers. comm.). The time scale for melting the terrestrial ice sheets and the consequent sea-level rise is more uncertain, at least a millennium if the ice was 10 times thicker (2 km) than the terminal sea glacier (0.2 km, Goodman & Pierrehumbert, 2003) to begin with. Following millions of years of deep freeze, deglaciation was cataclysmic. With a pCO_2 of $\sim$0.2 bar needed to deglaciate a Neoproterozoic snowball Earth (Caldeira & Kasting, 1992), tropical sea surface temperatures were raised to $\sim$50 °C (R.T. Pierrehumbert, pers. comm.) in the greenhouse aftermath. Intense carbonate (dolomite) weathering delivered alkalinity to the ocean and drove the precipitation of cap dolostone on the time scale of the post-glacial transgression (Higgins & Schrag, 2003). Rapid melting and surface warming imposed severe density stratification on ocean waters, impeding mixing between the oxic, brackish, surface water and euxinic, saline, hydrothermally dominated, deep water.

Sturtian glaciation in Svalbard?

If the Polarisbreen diamictites jointly represent the Marinoan glaciation in Svalbard (Fig. 14), then where in the underlying Hecla Hoek stratigraphy is the older Sturtian global glaciation (Knoll, 2000)? No older glacial deposits have been found (and may never be given the limited area of exposure), but perhaps this is not surprising considering that the vast conformable succession of shallow-water carbonates would have provided no topography for glacial nucleation. Glacial deposits are largely absent from the Marinoan-age carbonate platform in Namibia for that reason, but are found on the upper continental slope (Hoffman *et al*., 1998b; Hoffman, 2002), a facies not encountered in Svalbard. Post-glacial cap carbonates, on the other hand, are transgressive and normally extend far beyond the limits of the related glacial deposits (Hoffman & Schrag, 2002).

Sturtian cap carbonates have characteristic features in Australia, Canada and Namibia (Kennedy *et al*., 1998),

which should facilitate its recognition in Svalbard in the absence of Sturtian glacial deposits. They are generally dark grey, regressive sequences that begin with argillaceous limestone containing allodapic beds or, less commonly, sublittoral microbial laminae. They are condensed, compared with Marinoan cap carbonates, and the transgressive tracts that host the declining arm of the $\delta^{13}C$ anomaly are generally missing. Consequently, $\delta^{13}C$ rises with stratigraphic height from -2‰ or lower at the base to highs of $+5$‰ (Kennedy *et al.*, 1998; McKirdy *et al.*, 2001; Yoshioka *et al.*, 2003) (Fig. 13). Hoffman & Schrag (2002) speculated that Sturtian seawater did not reach critical oversaturation with respect to $CaCO_3$ until after the postglacial transgression, and that the weathering flux of alkalinity was lower than in the Marinoan because less carbonate rock was available globally for submarine dissolution and weathering.

Even though negative $\delta^{13}C$ values occur within the Akademikerbreen carbonates (Knoll *et al.*, 1986; Kaufman *et al.*, 1997; Halverson *et al.*, 2003), we argue that the lower Russøya Member is the closest analog beneath the Petrovbreen diamictite to the Rasthof Formation cap carbonate. Like the Rasthof (Hoffman *et al.*, 1998; Kennedy, 1998), it comprises a single, shoaling-upward half-sequence that is relatively rich in organic matter and begins with deep-water, bluish-grey to black, argillaceous limestone, intercalated in some sections with thin dolomite beds. In the most carbonate-rich section (measured section 1) $\delta^{13}C$ rises from 1.5‰ to 5‰ in the lower half of the sequence. Allowing for poor exposure and lack of carbonate in the lowermost Russøya, the δ^{13} C profile matches that of the Rasthof Formation (Yoshioka *et al.*, 2003).

If the lower Russøya Member is a Sturtian cap carbonate, then based on characteristics of other equivalent cap carbonates, the glacial surface should be at the top of the Dartboard Dolomite (Fig. 4). The contact is poorly exposed, and sedimentologically, the Dartboard itself is as strange as its name. In fact, many of its distinctive features (isopachous sea-floor cements, macropeloids, wave-like bedforms, sublittoral microbial laminae) are similar to Marinoan cap dolostones. Most Sturtian cap carbonates lack transgressive cap dolostones and begin at the maximum flooding stage or later (Hoffman & Schrag, 2002), so why should a ^{13}C-enriched Sturtian cap dolostone appear in Svalbard (no equivalent is known in East Greenland)? It is tempting to speculate that platform waters over Svalbard reached critical oversaturation with respect to the dolomite precursor earlier than elsewhere because of a local source of alkalinity, which in this case would have been the strongly ^{13}C-enriched Akademikerbreen carbonate platform.

If the Dartboard Dolomite were the Sturtian cap dolostone, by analogy to Marinoan cap dolostones, its base should be the glacial surface. Unfortunately, the base of the Dartboard is no better exposed than the top, and no obvious sequence boundary has been identified at this stratigraphic level. The variable depth of deposition, from sublittoral (Knoll *et al.*, 1989) to shallow/intermittently exposed, implied by the range in facies in the Dartboard Dolomite, suggests significant relief on this contact. On the other hand, the top of the Dartboard Dolomite is locally brecciated (Fairchild & Hambrey, 1984), and absent altogether in northernmost Spitsbergen, leaving opening the possibility that the Dartboard Dolomite, while lithologically similar to Marinoan-aged cap dolostones is not part of the Sturtian cap-carbonate sequence.

Irrespective of the origin and timing of the Dartboard dolomite, it is clear that the EGES platform experienced a profound change in depositional style in the uppermost Akademikerbreen Group (Herrington & Fairchild, 1989). Fairchild & Hambrey (1995) attributed the sudden influx of fine siliciclastic sediment in the underlying Kinnvikka Member (Fig. 4) and local deepening on the EGES platform to tectonic uplift. While tectonic uplift may have been a factor, the evidence for high-amplitude fluctuations in base level, including the development in measured section 10 of a 45 m-high, pinnacle reef with multiple debris aprons, is highly suggestive of a glacioeustatic oscillation. An alternative explanation for the influx of fine clastic sediment in the Kinnvikka Member could be transient landscape disequilibrium associated with climatic deterioration during the incipient Sturtian glaciation (Zhang *et al.*, 2001).

The hypothesis that the base of the Polarisbreen Group (Russøya Member) is the cap carbonate to a cryptic Sturtian glaciation is speculative, and we regard the problem of the Sturtian glaciation on the EGES platform as unresolved. We cannot rule out that the Sturtian glaciation is represented either in the underlying Akademikerbreen Group or by the Petrovbreen Member, but global correlations that will be developed in a separate paper render these options less likely. The potential key interval (Kinnvikka–Dartboard–lower Russøya) is exposed in an unexplored area directly west of the Vestfonna Ice Dome on Nordaustlandet (Fig. 1).

CONCLUSIONS

The Neoproterozoic Polarisbreen Group of northeastern Svalbard contains two diamictite-rich units, the older Petrovbreen Member and the younger Wilsonbreen Formation, that are conventionally interpreted to represent two distinct glaciations. The Petrovbreen diamictites are oligomictic, derived from directly underlying carbonates of the Russøya Member, and thinner overall than the Wilsonbreen diamictites, which are polymictic and include extrabasinal basement material. A well-defined, 10‰, negative $\delta^{13}C$ anomaly occurs in the Russøya Member directly beneath the erosion surface on which the Petrovbreen diamictites were deposited. This anomaly is homologous (Fig. 13) with those observed beneath the Elatina glacials in South Australia (McKirdy *et al.*, 2001), the Ghaub glacials in northern Namibia (Halverson *et al.*, 2002), and the Stelfox glacials in northwestern Canada (Hoffman & Schrag, 2002), all of which are correlated with the Marinoan glaciation in the South Australian type section (Kennedy *et al.*, 1998; Hoffman & Schrag, 2002). The

Petrovbreen diamictites have no well-developed post-glacial cap carbonate, but the younger Wilsonbreen diamictites have a cap dolostone (basal Dracoisen Formation) that is similar compositionally, sedimentologically and isotopically (Fig. 13) to Marinoan-age cap dolostones in Australia (Kennedy, 1996), Canada (James *et al*., 2001) and Namibia (Hoffman & Schrag, 2002). Thus, from the perspective of the bounding strata and global correlations, the two diamictite-rich units in Svalbard appear to represent the beginning and end of a single Marinoan glacial cycle.

We propose a new interpretation of the glacial history of the EGES platform that is consistent with these correlations and with the snowball Earth hypothesis for the Marinoan glaciation. In Polarisbreen times, the EGES marine platform was situated in the subtropics of the southern hemisphere on the south-facing margin of Laurentia, represented by the hinterland of present-day East Greenland. Carbonate sedimentation of the Russøya Member ended with a >50 m base-level drop that heralded the glaciation. Adjacent to the platform in East Greenland, an ice dome built up with cold-based ice descending to tidewater. The ice dome deposited thick tills at the ice front and released debris-laden icebergs that rafted the veneer of Petrovbreen glacimarine diamictite across the platform. Overlying the ice-rafted debris is a thick unit (MacDonaldryggen Member) of finely laminated suspension deposits that lack dropstones but are speckled with calcite pseudomorphs that we interpret to be glendonites. We regard the Petrovbreen–MacDonaldryggen contact as the onset of the full-blown snowball Earth, when 'sea glaciers' (thick floating marine ice that flows toward the zone of melting or ablation) invaded the tropical oceans (Goodman & Pierrehumbert, 2003). The flux of ice-rafted debris disappeared when 'sikussak' ice (multi-annual, shorefast, sea ice) choked the EGES platform. The sikussak backstopped the ice dome and prevented calving, and may itself have been pinned to the platform by the sea glacier impinging on the shelf edge. The MacDonaldryggen suspension deposits accumulated beneath the sikussak ice from hypopycnal plumes and density flows issuing from ice streams beneath the slowly growing ice dome.

As the snowball Earth gradually warmed (because weathering could not keep pace with CO_2 outgassing), vapour transport increased and the global sea glacier flowed more rapidly. Inflow of sea ice from higher latitudes maintained thick ice on the tropical ocean even after sea-surface temperatures reached the melting point. The shorefast sikussak ice, however, melted away, leaving an oasis of open water over the EGES and other subtropical marine platforms and inland seas, while the world ocean remained ice covered. We interpret the Slangen Member, a regressive sabkha-like evaporitic dolomite sequence overlying the MacDonaldryggen Member, to be the sediment deposited in this oasis on the snowball Earth. Opening of the EGES oasis led to rapid expansion of the downwind ice dome, which advanced across the shelf and deposited the Wilsonbreen ice-contact deposits. In front of the advancing ice, sands of the Bråvika Member were redeposited by outwash streams. The Wilsonbreen ice sheet had advanced almost to the present northern limit of the Polarisbreen outcrop belt when, in our interpretation, the sea glaciers finally collapsed, leading to cataclysmic deglaciation and attendant sea level rise. The basal Dracoisen cap dolostone is the signature of this transgression. Ironically, our interpretation associates the full-blown snowball Earth with two units that are not overtly glacial in origin, the MacDonaldryggen Member suspension deposits and the Slangen Member sabkha cycle.

If both diamictite-rich units in Svalbard belong to the Marinoan glaciation, the older Sturtian glaciation should be represented in the underlying strata (Knoll, 2000). No glacial deposits are known beneath the Petrovbreen/Ulvesø diamictites. This is perhaps not surprising considering the conformable nature of the vast, shallow-marine, carbonate platform (Akademikerbreen Group), which would provide no topography on which terrestrial glaciers might nucleate. However, a possible Sturtian cap-carbonate sequence is found in the lower Russøya Member, which is sedimentologically similar to the Rasthof Formation in Namibia (Hoffmann and Prave, 1996; Hoffman *et al*., 1998; Kennedy *et al*., 1998; Yoshioka *et al*., 2003). The basal Russøya Member lacks a negative $\delta^{13}C$ anomaly, but it shows a positive $\delta^{13}C$ trend like that of other Sturtian cap carbonates (Kennedy *et al*., 1998).

Evidence for open water on shallow platforms during the Marinoan glaciation has been reported in other regions (e.g., Williams, 1996; Prave, 1999; Williams & Schmidt, 2000; Kennedy *et al*., 2001; Condon *et al*., 2002). Since Kirschvink (1992), this evidence has always been cited in opposition to the snowball hypothesis. We conclude the opposite, that shorefast sea ice in the relatively ablative subtropics should melt away, exposing seawater on shallow shelves and inland seas, well before the global sea glacier finally collapsed. Oases should develop as a natural consequence of the snowball cycle, and they highlight the role of sea glaciers in the critical phases of the cycle (Goodman & Pierrehumbert, 2003). More generally, they remind us that while the Neoproterozoic stratigraphic records we rely on are epicontinental, the snowball Earth cycle is fundamentally an oceanographic phenomenon.

SUPPLEMENTARY MATERIAL

The following material is available from:
http://www.blackwellpublishing.com/products/journals/suppmat/BRE/BRE234/BRE234sm.htm

Appendix A1 Data table of $\delta^{13}C$ and $\delta^{18}O$ data presented in this paper.

ACKNOWLEDGMENTS

This work was supported by the National Science Foundation (Arctic Science Program grant OPP-9817244), the NASA Astrobiology Institute, the Canadian Institute

for Advanced Research (Earth System Evolution Project), and a GSA graduate research grant. Norsk Polarinstitutt provided logistical support in Svalbard, and Winfried Dallman helped us greatly in organizing our field work. We thank Dan Schrag for use of his laboratory and many discussions about the data in this paper. Ian Fairchild, Peter DeCelles, and an anonymous referee provided excellent reviews that greatly improved this paper, as did comments by Andy Knoll on an earlier draft. We thank Sam Bowring, Dan Condon, Jason Goodman, John Grotzinger, Matt Hurtgen, Stein Jacobsen, Jay Kaufman, Peter Moore, Ray Pierrehumbert, Susannah Porter, Pascale Poussart, and Steve Warren for valuable discussions. Cris Carman, Anne Estoppey, John Higgins, Leslie Hsu, Brice Jones, Peter Moore, and Meg Smith, provided field assistance. Ethan Goddard and Greg Escheid supervised the laboratory work.

REFERENCES

Aitken, J.D. (1991) The Ice Brook Formation and Post-Rapitan, Late Proterozoic glaciation, Mackenzie Mountains, Northwest Territories. *Geol. Surv. Canada Bull.*, **404**, 43pp.

Allan, J.R. & Matthews, R.K. (1982) Isotope signatures associated with early meteoric diagenesis. *Sedimentology*, **29**, 797–817.

Alley, R.B., Blankenshio, D.D., Rooney, S.T. & Bentley, C.R. (1989) Sedimentation beneath ice shelves – the view from Ice Stream B. *Marine Geology*, **85**, 101–120.

Anderson, J.B. (1999) *Antarctic Marine Geology*. Cambridge University Press, Cambridge, UK, 289pp.

Asmeron, Y., Jacobsen, S.B., Knoll, A.H., Butterfield, N.J. & Swett, K. (1991) Strontium isotopic variations of Neoproterozoic seawater: implications for crustal evolution. *Geochim. Cosmochim. Acta*, **55**, 2883–2894.

Atkins, C.B., Barrett, P.J. & Hicock, S.R. (2002) Cold glaciers erode and deposit: evidence from Allan Hills, Antarctica. *Geology*, **30**(7), 659–662.

Banner, J.L. & Hanson, G.N. (1990) Calculation of simultaneous isotopic and trace element variations during water-rock interaction with applications to carbonate diagenesis. *Geochim. Cosmochim. Acta*, **54**, 3123–3137.

Boggs, S. Jr. (1972) Petrography and geochemistry of rhombic, calcite pseudomorphs from mid-Tertiary mudstones of the Pacific Northwest, U.S.A. *Sedimentology*, **19**, 219–235.

Bowring, S., Myrow, P., Landing, E., Ramezani, J. & Grotzinger, J. (2003) Geochronological constraints on terminal Proterozoic events and the rise of Metazoans. *Geophys. Res. Abstr. (EGS, Nice)* **5**, 13219.

Brand, U. & Veizer, J. (1980) Chemical diagenesis of a multicomponent carbonate system -1: trace elements. *J. Sediment. Petrol.*, **50**, 1219–1236.

Brand, U. & Veizer, J. (1981) Chemical diagenesis of a multicomponent carbonate system -2: stable isotopes. *J. Sediment. Petrol.*, **51**, 987–997.

Brasier, M.D. & Shields, G. (2000) Neoproterozoic chemostratigraphy and correlation of the Port Askaig glaciation, Dalradian Supergroup of Scotland. *J. Geol. Soc. London*, **157**, 909–914.

Buchan, K.L., Mertanen, S., Park, R.G., Pesonen, L.J., Elming, S.-Å., Abrahamsen, N. & Bylund, G. (2000) Comparing the drift of Laurentia and Baltica in the Proterozoic: the importance of key palaeomagnetic poles. *Tectonophysics*, **319**, 167–198.

Buchart, B., Seaman, P., Stockmann, G., Vous, M., Wilken, U., Duwel, L., Kriastiansen, A., Jenner, C., Whiticar, M.J., Kristensen, R.M., Petersen, G.H. & Thorbjorn, L. (1997) Submarine columns of ikaite tufa. *Nature*, **390**, 129–130.

Budyko, M.I. (1969) The effect of solar radiation variations on the climate of the Earth. *Tellus*, **21**, 611–619.

Butterfield, N.J., Knoll, A.H. & Swett, K. (1994) Paleobiology of the Neoproterozoic Svanbergfjellet Formation, Spitsbergen. *Fossils Strata*, **34**, 1–84.

Caldeira, K. & Kasting, J.F. (1992) Susceptibility of the early Earth to irreversible glaciation caused by carbon dioxide clouds. *Nature*, **359**, 226–228.

Calver, C.R. (2000) Isotope stratigraphy of the Ediacarian (Neoproterozoic III) of the Adelaide Rift Complex, Australia, and the overprint of water column stratification. *Precambrian Res.*, **100**, 121–150.

Carey, S.W. & Ahmad, N. (1961) Glacial marine sedimentation. In: *Geology of the Arctic* (Ed. by G.O. Raasch), pp. 865–894. University of Toronto Press, Toronto.

Chafetz, H.S., Imerito-Teizlaff, A.A. & Zhang, J. (1999) Stable-isotope and elemental trends in Pleistocene sabkha dolomites: descending meteoric water vs. sulfate reduction. *J. Sediment. Res.*, **69**, 256–266.

Chumakov, N.M. (1968) On the character of the Late Precambrian glaciation of Spitsbergen (translated title). *Dokl. Akad Nauk SSSR, Ser. Geol.*, **180**, 1446–1449.

Chumakov, N.M. (1978) *Precambrian tillites and tilloids (translated title)*. 72–87. Nauka, Moscow (in Russian).

Condon, D.J., Prave, A.R. & Benn, D.I. (2002) Neoproterozoic glacial-rain out intervals: observations and implications. *Geology*, **30**, 35–38.

Cotter, K.L. (1999) Microfossils from Neoproterozoic Supersequence 1 of the Officer Basin, Western Australia. *Alcheringa*, **23**, 63–86.

Council, T.C. & Bennett, P.C. (1993) Geochemistry of ikaite formation at Mono Lake, California: implications for the origin of tufa mounds. *Geology*, **21**, 971–974.

Cuffey, K.M., Conway, H., Gades, A.M., Hallet, B., Lorrain, R., Severinghaus, J.P., Steig, E.J, Vaughn, B. & White, J.W.C. (2000) Entrainment at cold glacier beds. *Geology*, **28**(4), 351–354.

De Angelis, H. & Skvarca, P. (2003) Glacier surge after ice shelf collapse. *Science*, **299**, 1560–1562.

De Lurio, J.L. & Frakes, L.A. (1999) Glendonites as a paleoenvironmental tool: implications for early Cretaceous high latitude climates in Australia. *Geochim. Cosmochim. Acta*, **63**, 1039–1048.

Derry, L.A., Kaufman, A.J. & Jacobsen, S.B. (1992) Sedimentary cycling and environmental change in the Late Proterozoic: evidence from stable and radiogenic isotopes. *Geochim. Cosmochim. Acta*, **56**, 1317–1329.

Des Marais, D.J. & Moore, J.G. (1984) Carbon and its isotopes in mid-oceanic basaltic glasses. *Earth Planet. Sci. Lett.*, **69**, 43–57.

Dewey, J.F. & Strachan, R.A. (2003) Changing Silurian–Devonian relative plate motion in the Caledonides: sinistral transpression to sinistral transtension. *J. Geol. Soc. London*, **160**, 219–229.

Donnadieu, Y., Fluteau, F., Ramstein, G., Ritz, C. & Besse, J. (2003) Is there a conflict between Neoproterozoic glacial

deposits and the snowball Earth interpretation: an improved understanding with numerical modeling. *Earth Planet. Sci. Let.*, **208**, 101–112.

Dowdeswell, J.A., Elverhøi, A. & Spielhagen, R. (1998) Glacimarine sedimentary processes and facies on the polar North Atlantic Margins, *Quat. Sci. Rev.*, **17**, 243–272.

Dowdeswell, J.A., Whittington, J.A., Jennings, A.E., Andrews, J.T., Mackensen, A. & Marienfield, P. (2000) An origin for laminated glacimarine sediments through sea-ice build-up and suppressed iceberg rafting. *Sedimentology*, **47**, 557–576.

Dowdeswell, J.A., Hambrey, M.J. & Wu, R. (1985) A Comparison of clast fabric and shape in Late Precambrian and Modern glacigenic sediments. *J. Sediment. Petrol.*, **55**(5), 691–704.

Drewry, D.J. & Cooper, A.P.R. (1981) Processes and models of Antarctic glacimarine sedimentation. *Ann. Glaciol.*, **2**, 117–122.

Elverhøi, A., Pfirman, S.L., Solheim, A. & Larssen, B.B. (1989) Glacimarine sedimentation in epicontinental seas exemplified by the Northern Barents Sea. *Mar. Geol.*, **85**, 225–250.

Embleton, B.J.J. & Williams, G.E. (1986) Low palaeolatitude of deposition for late Precambrian periglacial varvites in South Australia: implications for palaeoclimatology. *Earth Planet. Sci. Lett.*, **79**, 419–430.

Evans, D.A.D. (2000) Stratigraphic, geochronological, and paleomagnetic constraints upon the Neoproterozoic climatic paradoxes. *Am. J. Sci.*, **300**, 347–443.

Fairchild, I.J. (1993) Balmy shores and icy wastes: the paradox of carbonates associated with glacial deposits in Neoproterozoic times. In: *Sedimentology Review 1* (Ed. by V.P. Wright), pp. 1–16. Blackwell Scientific Publications, Oxford, UK.

Fairchild, I.J. & Hambrey, M.J. (1984) The Vendian succession of northeastern Spitsbergen: petrogenesis of a dolomite-tillite association. *Precambrian Res.*, **26**, 111–167.

Fairchild, I.J. & Hambrey, M.J. (1995) Vendian basin evolution in East Greenland and NE Svalbard. *Precambrian Res.*, **73**, 217–233.

Fairchild, I.J., Hambrey, M.J., Spiro, B. & Jefferson, T.H. (1989) Late Proterozoic glacial carbonates in northeast Spitsbergen: new insights into the carbonate-tillite association. *Geol. Mag.*, **126**, 469–490.

Fairchild, I.J. & Spiro, B. (1987) Petrological and isotopic implications of some contrasting Late Precambrian carbonates, NE Spitsbergen. *Sedimentology*, **34**, 973–989.

Fairchild, I.J. & Spiro, B. (1990) Carbonate minerals in glacial sediments: geochemical clues to palaeoenvironment. In: *Glacimarine Environments: Processes and Sediments* (Ed. by J.A. Dowdeswell & J.D. Scourse), *Geol. Soc. Spec. Publ.*, **53**, 201–216.

Fairchild, I.J., Spiro, B., Herrington, P.M. & Song, T. (2000) Controls on Sr and C isotope compositions of Neoproterozoic Sr-rich limestones of East Greenland and North China. In: *Carbonate Sedimentation in the Evolving Precambrian World* (Ed. by J.P. Grotzinger & N.P. James), *SEPM Spec. Publ.*, **67**, 297–313.

Frederiksen, K.S., Craig, L.E. & Skipper, C.B. (1999) New observations of the stratigraphy and sedimentology of the Upper Proterozoic Andrée Land Group, East Greenland: supporting evidence for a drowned carbonate ramp. In: *Geology of East Greenland 72°–75°N, mainly Caledonian: preliminary reports from the 1998 expedition, Danmarks og Grønlands Geologiske Undersøgelse Rapport 1999/19* (Ed. by A.K. Higgins & K.S. Frederiksen), pp. 145–158. Geological Survey of Denmark, Copenhagen.

Friedman, I. & O'Neil, J.R. (1977) Compilation of stable isotope fractionation factors of geochemical interest. *US Geol. Surv. Prof. Pap.*, **440-KK**, 49p.

Funder, S., Hjort, C., Landvik, J.Y., Nam, S., Reeh, N. & Stein, R. (1998) History of a stable ice margin – East Greenland during the Middle and Upper Pleistocene. *Quat. Sci. Rev.*, **17**, 77–123.

Gee, D.G. & Page, L.M. (1994) Caledonian terrane assembly on Svalbard: new evidence from $^{40}Ar/^{39}Ar$ dating in Ny Friesland. *Am. J. Sci.*, **294**, 1166–1186.

Gee, D.G., Johansson, Å., Ohta, Y., Tebenkov, A.M., Krasilyshchivov, A.A., Balashov, Y.A., Larianov, A.N., Gannibal, L.F. & Ryungenen, G.I. (1995) Grenvillian basement and a major unconformity within the Caledonides of Nordaustlandet, Svalbard. *Precambrian Res.*, **70**, 215–234.

Gildor, H. & Tziperman, E. (2000) Sea ice as the glacial cycles' climate switch; the role of seasonal and orbital forcing. *Paleoceanography*, **15**(6), 605–615.

Goodman, J.C. & Pierrehumbert, R.T. (2003) Glacial flow of floating marine ice in 'Snowball Earth'. *J. Geophys. Res.*, **108 (C10)**, 3308, 0.1029/2002JC001471.

Grotzinger, J.P. & Knoll, A.H. (1995) Anomalous carbonate precipitates: is the Precambrian the key to the Permian? *Palaios*, **10**, 578–596.

Halverson, G.P. (2003) Towards an integrated stratigraphic and carbon-isotopic record for the Neoproterozoic. PhD Thesis, Harvard University, Cambridge, MA, USA, 276pp.

Halverson, G.P., Hoffman, P.F., Maloof, A.C. & Rice, A.H. (2003) Towards a composite carbon isotopic curve for the Neoproterozoic. (Abstract). *Conference Proceedings of the IV South American Symposium on Isotope Geology*, Salvador, Brazil, pp. 14–17.

Halverson, G.P., Hoffman, P.F., Schrag, D.P. & Kaufman, A.J. (2002) A major perturbation of the carbon cycle before the Ghaub glaciation (Neoproterozoic) in Namibia: prelude to snowball Earth? *Geochem., Geophys., Geosyst.*, **3**, 10.1029/2001GC000244.

Hambrey, M.J. (1982) Late Precambrian diamictites of northeastern Svalbard. *Geol. Mag.*, **119**, 527–551.

Hambrey, M.J. (1983) Correlation of late Proterozoic tillites in the North Atlantic region and Europe. *Geol. Mag.*, **120**, 290–320.M

Hambrey, M.J. & Spencer, A.M. (1987) Late Precambrian glaciation of Central East Greenland. *Meddelelser om Grønland*, **19**, 50pp.

Harland, W.B. (1997) *The Geology of Svalbard Geol. Soc. London Mem.*, **17**, 521pp.

Harland, W.B. & Gayer, R.A. (1972) The Arctic Caledonides and earlier oceans. *Geol. Mag.*, **109**, 289–314.

Harland, W.B., Hambrey, M.J. & Waddams, P. (1993) Vendian Geology of Svalbard. *Norsk. Polarinst. Skr.*, **193**, 150pp.

Harland, W.B. & Wilson, C.B. (1956) The Hecla Hoek succession in Ny Friesland, Spitsbergen. *Geol. Mag.*, **93**, 265–286.

Harland, W.B., Scott, R.A., Aukland, K.A. & Snape, I. (1992) The Ny Friesland Orogen, Spitsbergen. *Geol. Mag.*, **129**, 679–707.

Hartz, E.H. & Torsvik, T.H. (2002) Baltica upside down: a new plate tectonic model for Rodinia and the Iapetus Ocean. *Geology*, **30**, 255–258.

Heaman, L.M., LeCheminant, A.N. & Rainbird, R.H. (1992) Nature and timing of Franklin igneous events, Canada: implications for a Late Proterozoic mantle plume and the breakup of Laurentia. *Earth Planet. Sci. Lett.*, **109**, 117–131.

Henriksen, N. (1981) The Charcot Land tillite, Scoresby Sund, East Greenland. In: *Earth's Pre-Pleistocene Glacial Record* (Ed. by M.J. Hambrey & W.B. Harland), pp. 776–777. Cambridge University Press, Cambridge.

Henriksen, N. & Higgins, A.K. (1976) East Greenland Caledonian fold belt. In: *Geology of Greenland* (Ed. by A. Escher & W.S. Watt) Greenland Geological Survey, Copenhagen.

Herrington, P.M. & Fairchild, I.J. (1989) Carbonate shelf and slope facies evolution prior to Vendian glaciation, central East Greenland. In: *The Caledonide Geology of Scandinavia* (Ed. by R.A. Gayer), pp. 285–297. Graham Trotman, London.

Higgins, A.K. (1981) The Late Precambrian Tillite Group of the Kong Oscars Fjord and Kejser Franz Josefs Fjord region of East Greenland. In: *Earth's Pre-Pleistocene Glacial Record* (Ed by M.J. Hambrey & W.B. Harland), pp. 778–781. Cambridge University Press, Cambridge.

Higgins, A.K., Leslie, A.G. & Smith, M.P. (2001) Neoproterozoic–Lower Palaeozoic stratigraphical relationships in the marginal thin-skinned thrust belt of the East Greenland Caledonides: comparisons with the foreland in Scotland. *Geol. Mag.*, **138**(2), 143–160.

Higgins, J.A. & Schrag, D.P. (2003) The aftermath of a snowball Earth. *Geochem., Geophys., Geosyst.*, **4**(3), 1028. doi:10.1029/2002GC000403, 2003.

Hill, A.C., Arouri, K., Gorjan, P. & Walter, M.R. (2000) Geochemistry of marine and nonmarine environments of a Neoproterozoic cratonic carbonate/evaporite: the Bitter Springs Formation, Central Australia. In: *Carbonate Sedimentation and Diagenesis in an Evolving Precambrian World* (Ed. by J.P. Grotzinger & N.P. James), *SEPM Spec. Publ.*, **67**, 327–344.

Hill, A.C. & Walter, M.R. (2000) Mid-Neoproterozoic (~830–750 Ma) isotope stratigraphy of Australia and global correlation. *Precambrian Res.*, **100**, 181–211.

Hoffman, P.F. (2002) *Carbonates Bounding Glacial Deposits: Evidence for Snowball Earth Episodes and Greenhouse Aftermaths in the Neoproterozoic Otavi Group of Northern Namibia*. International Association of Sedimentologists, Field Excursion Guidebook. Auckland Park, South Africa, pp. 1–49.

Hoffmann, K.H. & Prave, A.R. (1996) A preliminary note on a revised subdivision and regional correlation of the Otavi Group based on glaciogenic diamictites and associated cap dolostones. *Commun. Geol. Soc. Namibia*, **11**, 81–86.

Hoffman, P.F., Kaufman, A.J., Halverson, G.P. & Schrag, D.P. (1998) A Neoproterozoic snowball Earth. *Science*, **281**, 1342–1346.

Hoffman, P.F. & Schrag, D.P. (2002) The snowball Earth hypothesis: testing the limits of global change. *Terra Nova*, **14**, 129–155.

Hoffman, P.F., van Dusen, A., Halverson, G.P., Saenz, J., Kaufman, A.J. & Schrag, D.P. (2002) Significance of seafloor barite cements in Marinoan-aged post-glacial cap carbonates (abstract). *Goldschmidt Conference Proceedings*, Davos, A847.

Irwin, H., Curtis, C. & Coleman, M. (1977) Isotopic evidence for source of diagenetic carbonates formed during burial of organic-rich sediments. *Nature*, **269**, 209–213.

Jacobsen, S.B. & Kaufman, A.J. (1999) The Sr, C, and O isotopic evolution of Neoproterozoic seawater. *Chem. Geol.*, **161**, 37–57.

James, N.P., Narbonne, G.M. & Kyser, T.K. (2001) Late Neoproterozoic cap carbonates: Mackenzie Mountains, northwestern Canada: precipitation and global glaciation. *Can. J. Earth Sci.*, **38**, 1229–1262.

Johannson, Å., Larianov, A.N., Tebenkov, A.M., Gee, D.G., Whitehouse, M.J. & Vestin, J. 2000 Grenvillian magmatism of western and central Nordaustlandet, northeastern Svalbard. *Trans. R. Soc. Edinburgh*, **90**, 221–234.

Kamo, S.L. & Gower, C. (1994) Note: U–Pb baddeleyite dating clarifies age of characteristic paleomagnetic remanence of Long Range dykes, southeastern Labrador. *Atlantic Geol.*, **30**, 259–262.

Katz, H.R. (1960) Late Precambrian to Cambrian stratigraphy in East Greenland. In *Geology of the Arctic: Proceedings of the First International Symposium on Arctic Geology* (Ed by G.O. Raasch), 299–328. Toronto University Press, Toronto.

Kaufman, A.J., Knoll, A.H. & Narbonne, G.M. (1997) Isotopes, ice ages, and terminal Proterozoic earth history. *Proc. Natl. Acad. Sci.*, **94**, 6600–6605.

Kemper, E. & Schmitz, H.H. (1981) Glendonite-Indikatoren des Polarmarinen Abagerungsmilieus. *Geol. Rundsch*, **70**, 759–773.

Kendall, C.G.St.C. & Skipwith, P.A.d'E. (1969) Holocene shallow water carbonate and evaporite sediments of Khor al Bazam, abu Dhabi, South West Persion Gulf. Bull. *Am. Assoc. Petrol. Geol.*, **53**, 841–869.

Kendall, C.G.St.C. & Warren, J. (1987) A review of the origin and setting of tepees and their associated fabrics. *Sedimentology*, **34**, 1007–1027.

Kennedy, M.J. (1996) Stratigraphy, sedimentology, and isotopic geochemistry of Australian Neoproterozoic postglacial cap dolostones: Deglaciation, $\delta^{13}C$ excursions, and carbonate precipitation. *J. Sediment. Res.*, **66**, 1050–1064.

Kennedy, M.J., Christie-Blick, N. & Sohl, L.E. (2001) Carbon isotopic composition of Neoproterozoic glacial carbonates as a test of paleoceanographic models for snowball Earth phenomena. *Geology*, **29**, 1135–1138.

Kennedy, M.J., Runnegar, B., Prave, A.R., Hoffman, K.H. & Arthur, M. (1998) Two or four Neoproterozoic glaciations? *Geology*, **26**, 1059–1063.

Kennedy, S.K., Hopkins, D.M. & Pickthorn, W.J. (1987) Ikaite, the glendonite precursor, in estuarine sediments at Barrow, Arctic Alaska. *GSA Abstr. Programs*, **19**(7), 725.

Kirschvink, J.L. (1992) Late Proterozoic low latitude glaciation: the snowball earth. In: *The Proterozoic Biosphere: A Multidisciplinary Study* (Ed by J.W. Schopf & C. Klein), pp. 51–52. Cambridge University Press, Cambridge.

Klein, C. & Beukes, N.J. (1993) Sedimentology and geochemistry of the glaciogenic late Proterozoic Rapitan iron-formation in Canada. *Econ. Geol.*, **84**, 1733–1774.

Knoll, A.H. (2000) Learning to tell Neoproterozoic time. *Precambrian Res.*, **100**, 3–20.

Knoll, A.H., Hayes, J.M., Kaufman, A.J., Swett, K. & Lambert, I.B. (1986) Secular variation in carbon isotope ratios from Upper Proterozoic successions of Svalbard and east Greenland. *Nature*, **321**, 832–837.

Knoll, A.H. & Swett, K. (1987) Micropaleontology across the Precambrian–Cambrian boundary in Spitsbergen. *J. Palaeontol.*, **61**, 898–926.

Knoll, A.H. & Swett, K. (1990) Carbonate deposition during the Late Proterozoic era: an example from Spitsbergen. *Am. J. Sci.*, **290-A**, 104–132.

Knoll, A.H., Swett, K. & Burkhart, E. (1989) Paleoenvironmental distribution of microfossils and stromatolites in the Upper Proterozoic Backlundtoppen Formation, Spitsbergen. *J. Paleontol.*, **63**, 129–145.

Knoll, A.H., Swett, K. & Mark, J. (1991) Paleobiology of a Neoproterozoic tidal flat lagoon complex: the Draken Conglomerate Formation, Spitsbergen. *J. Paleontol.*, **65**, 531–569.

Koch, L. (1945) The East Greenland ice. *Meddelelser om Grønland*, **130**, 1–373.

Kulling, O. (1934) Scientific results of the Swedish–Norwegian arctic expedition in the summer of 1931. *Geogr. Annlr. Stockh.*, **16**, 161–253.

Larianov, A., Gee, D.G., Tebenkov, A.M. & Witt-Nillson, P. (1998) Detrital zircon ages from the Planetfjella Group of the Mosselhalvøya Nappe, NE Spitsbergen, Svalbard. *International Conference on Arctic Margins*, III, Celle, Germany, pp. 109–110.

Lewis, J.P., Weaver, A.J., Johnston, S.T. & Eby, M. (2003) The Neoproterozoic 'Snowball Earth': dynamic sea ice over a quiescent ocean. *Paleoceanography*, **18**(4), 10.1029/2003PA000926.

Lyberis, N. & Manby, G. (1999) Continental collision and lateral escape deformation in the lower and upper crust: an example from Caledonide Svalbard. *Tectonics*, **18**, 40–63.

MacAyeal, D.R. (1993) A low-order model of the Heinrich Event cycle. *Palaeoceanograph*, **8**, 767–773.

McKay, C.P., Clow, G.D., Wharton, R.A. Jr & Squyres, S.W. (1985) Thickness of ice on perennially frozen lakes. *Nature*, **313**, 561–562.

McKirdy, D.M., Burgess, J.M., Lemon, N.M., Yu, X., Cooper, A.M., Gostin, V.A., Jenkins, R.J.F. & Both, R.A. (2001) A chemostratigraphic overview of the late Cryogenian interglacial sequence in the Adelaide Fold-Thrust Belt, South Australia. *Precambrian Res.*, **106**, 149–186.

Moncrieff, A.C.M. (1989) The Tillite Group and related rocks of East Greenland: implications for Late Proterozoic palaeogeography. In: *The Caledonian Geology of Scandinavia* (Ed. by R.A. Gayer), pp. 285–297. Graham & Trotman, London.

Moncrieff, A.C.M. & Hambrey, M.J. (1988) Late Precambrian glacially-related grooved and striated surfaces in the Tillite Group of Central East Greenland. *Paleogeogr., Paleoclimat., Paleoecol.*, **65**, 183–200.

Moncrieff, A.M. & Hambrey, M.J. (1990) Marginal-marine glacial sedimentation in the late Precambrian succession of East Greenland. In: *Glacimarine Environments: Processes and Sediments* (Ed. by J.A. Dowdeswell & J.D. Scourse), *Geol. Soc. London*, **Special Publication 53**, 387–410.

Morrow, D.W. & Ricketts, B.D. (1986) Chemical controls on the precipitation of mineral analogues of dolomite: the sulfate enigma. *Geology*, **16**, 408–410.

Murthy, G., Gower, C., Tubrett, M. & Patzold, R. (1992) Paleomagnetism of Eocambrian Long Range dykes and Double Mer Formation from Labrador, Canada. *Can. J. Earth Sci.*, **29**, 1224–1234.

Myrow, P. & Kaufman, A.J. (1998) A newly-discovered cap carbonate above Varanger age glacial deposits in Newfoundland, Canada. *J. Sediment. Res.*, **69**, 784–793.

Nogueira, A.C.R., Riccomini, C., Sial, A.N., Moura, C.A.V. & Fairchild, T.R. (2003) Soft-sediment deformation at the base of the Neoproterozoic Puga cap carbonate (southwestern Amazon craton, Brazil): confirmation of rapid icehouse–greenhouse transition in snowball Earth. *Geology*, **31**, 613–616.

Nystuen, J.P. (1985) Facies and preservation of glaciogenic sequences from the Varanger ice age in Scandinavia and other parts of the North Atlantic Region. *Palaeogeogr., Palaeoclimatol., Palaeoecol.*, **51**, 209–229.

Orheim, O. & Elverhøi, A. (1981) Model for submarine glacial deposition. *Ann. Glaciol.*, **2**, 123–128.

Payne, A.J. & Dongelmans, P.W. (1997) Self-organization in the thermomechanical flow of ice sheets. *J. Geophys. Res.*, **102**(B), 12,219–12,233.

Phillips, W.E.A. & Friderichsen, J.D. (1981) The Late Precambrian Gåseland tillite, Scoresby Sund, East Greenland. In: *Earth's Pre-Pleistocene Glacial Record* (Ed. by M.J. Hambrey & W.B. Harland), pp. 773–775. Cambridge University Press, Cambridge.

Pisarevksy, S.A., Wingate, T.D., Powell, C.McA., Johnson, S. & Evans, D.A.D. (2003) Models of Rodinia assembly and fragmentation. In: *Proterozoic East Gondwana: Supercontinental assembly and breakup* (Ed. by M. Yoshida, B.F. Windley, S. Dasgupta & C.McA. Powell), *Geol. Soc. London Spec. Publication*, **206**, 35–55.

Poulsen, C.J. (2003) Absence of a runaway ice-albedo feedback in the Neoproterozoic. *Geology*, **31**, 473–476.

Poulsen, C.J., Pierrehumbert, R.T. & Jacob, R.L. (2001) Impact of ocean dynamics on the simulation of the Neoproterozoic 'snowball Earth'. *Geophys. Res. Lett.*, **28**, 1575–1578.

Prave, A.R. (1999) Two diamictites, two cap carbonates, two $\delta^{13}C$ excursions, two rifts: the Neoproterozoic Kingston Peak Formation, Death Valley, California. *Geology*, **27**, 339–342.

Preiss, W.V. (2000) The Adelaide Geosyncline of South Australia and its significance in Neoproterozoic continental reconstruction. *Precambrian Res.*, **100**, 21–63.

Reimnitz, E., Kempema, E.W. & Barnes, P.W. (1987) Anchor ice, seabed freezing, and sediment dynamics in shallow Arctic seas. *J. Geophys. Res.*, **92**(C13), 14,671–14,678.

Schrag, D.P., Berner, R.A., Hoffman, P.F. & Halverson, G.P. (2002) On the initiation of a snowball Earth. *Geochem., Geophys., Geosyst.*, **3**, 10.1029/2001GC000219.

Sellers, W.D. (1969) A global climatic model based on the energy balance of the Earth–atmosphere system. *J. Appl. Meteorol.*, **8**, 392–400.

Schmidt, P.W. & Williams, G.E. (1995) The Neoproterozoic climatic paradox: equatorial paleolatitude for Marinoan glaciation near sea level in South Australia. *Earth Planet. Sci. Lett.*, **134**, 107–124.

Shields, G., Stille, P., Brasier, M.D. & Atudorei, N.-V. (1997) Stratified oceans and oxygenation of the late Precambrian environment: a post glacial geochemical record from the Neoproterozic of W. Mongolia. *Terra Nova*, **9**, 218–222.

Smith, M.P. & Robertson, S. (1999a) The Nathorst Land Group (Neoproterozoic) of East Greenland—lithostratigraphy, basin geometry, and tectonic history. In: *Geology of East Greenland 72°–75° N, Mainly Caledonian: Preliminary Reports from the 1998 Expedition, Danmarks og Grønlands Geologiske Undersøgelse Rapport 1999/19* (Ed. by A.K. Higgins & K.S. Frederiksen), pp. 127–142. Geological Survey of Denmark, Copenhagen.

Smith, M.P. & Robertson, S. (1999b) Vendian-Lower Palaeozoic stratigraphy of the parautochthon in the Målebjerg and Eleonore Sø thrust windows, East Greenland Caledonides. In: *Geology of East Greenland 72°–75° N, Mainly Caledonian: Preliminary Reports from the 1998 Expedition, Danmarks og Grønlands Geologiske Undersøgelse Rapport 1999/19* (Ed. by A.K. Higgins & K.S. Frederiksen), pp. 169–182. Geological Survey of Denmark, Copenhagen.

Soffer, G. (1998) Evolution of a Neoproterozoic continental margin subject to tropical glaciation. B.A. Thesis, Harvard College, Cambridge, MA, USA.

Sohl, L.E., Christie-Blick, N. & Kent, D.V. (1999) Paleomagnetic polarity reversals in Marinoan (ca. 600 Ma) glacial

deposits of Australia: implications for the duration of low-latitude glaciations in Neoproterozoic time. *Geol. Soc. Am. Bull.*, **111**, 1120–1139.

Sønderholm, M. & Tirsgaard, H. (1993) Lithostratigraphic framework of the Upper Proterozoic Eleonore Bay Supergroup of East and North-East Greenland. *Bull. Grønlands Geologiske Undersøgelse*, **167**, 38pp.

Spencer, A.M. (1985) Mechanisms and environments of deposition of Late Precambrian geosynclinal tillites: Scotland and East Greenland. *Palaeogeogr., Paleoclimatatol., Paleoecol.*, **51**, 143–157.

Suess, E., Balzer, W., Hesse, K.-F., Müller, P.J., Ungerer, C.A. & Wefer, G. (1982) Calcium carbonate hexahydrate from organic-rich sediments of the Antarctic Shelf: precursors of glendonites. *Science*, **216**, 1128–1131.

Swainson, I.P. & Hammond, R.P. (2001) Ikaite, $CaCO_3 \cdot 6H_2O$: cold comfort for glendonites as paleothermometers. *Am. Mineral.*, **86**, 1530–1533.

Torsvik, T.H., Smethurst, M.A., Meert, J.G., Van der Voo, R., McKerrow, W.S., Brasier, M.D., Sturt, B.A. & Walderhaug, H.J. (1996) Continental break-up and collision in the Neoproterozoic and Paleozoic – A tale of Baltica and Laurentia. *Earth-Sci. Rev.*, **40**, 229–258.

Walter, M.R., Veevers, J.J., Calvert, S.E., Gorjan, P. & Hill, A.C. (2000) Dating the 840–544 Ma Neoproterozoic interval by isotopes of strontium, carbon, and sulfur in seawater, and some interpretative models. *Precambrian Res.*, **100**, 371–433.

Warren, S.G., Brandt, R.E., Grenfell, T.C. & McKay, C.P. (2002) Snowball Earth: ice thickness on the tropical ocean. *J. Geophys. Res.*, **107**(C10), 3167.

Williams, G.E. (1979) Sedimentology, stable-isotope geochemistry and palaeoenvironment of dolostones capping late Precambrian glacial sequences in Australia. *Austr. J. Earth Sci.*, **26**, 377–386.

Williams, G.E. (1996) Soft-sediment deformation structures from the Marinoan glacial succession, Adelaide fold belt: implications for the paleolatitude of late Neoproterozoic glaciation. *Sediment. Geol.*, **106**, 165–175.

Williams, G.E. & Schmidt, P. (2000) Proterozoic equatorial glaciation: has 'snowball Earth' a snowball's chance? *Aust. Geol.*, **117**, 21–25.

Wilson, C.B. (1961) The upper Middle Hecla Hoek rocks of Ny Friesland, Spitsbergen. *Geol. Mag.*, **98**, 89–116.

Wilson, C.B. & Harland, W.B. (1964) The Polarisbreen Series and other evidences of late Pre-Cambrian ice ages in Spitsbergen. *Geol. Mag.*, **101**, 198–219.

Yoshioka, H., Asahara, Y., Tojo, B. & Kawakami, S. (2003) Systematic variations in C, O, and Sr isotopes and elemental concentrations in Neoproterozoic carbonates in Namibia: implications for glacial to interglacial transition. *Precambrian Res.*, **124**, 69–85.

Zhang, P., Molnar, P. & Downs, W.R. (2001) Increased sedimentation rates and grain sizes 2–4 Myr ago due to the influence of climate change on erosion rates. *Nature*, **410**, 891–897.

Manuscript received 20 August 2003; Manuscript Accepted: 21 April 2004

